Title
THE PSEUDO-FREE 32 VERTEX MODEL

Author
Samuel, Stuart.

Publication Date
1978-11-01

Submitted to Physical Review B

LBL-8427 c.2
Preprint

THE PSEUDO-FREE 32 VERTEX MODEL

Stuart Samuel

November 1978

Prepared for the U. S. Department of Energy
under Contract W-7405-ENG-48

DISCLAIMER

THE PSEUDO-FREE 32 VERTEX MODEL*

by

Stuart Samuel

Lawrence Berkeley Laboratory
University of California
Berkeley, California 94720

November 7, 1978

ABSTRACT

A new two-dimensional statistical mechanics model is solved. It is a general model with 18 free parameters and includes Ising-like spin systems and ferroelectric systems as subcases. The solution uses integrals over anticommuting variables.

*Supported by the High Energy Physics Division of the United States Department of Energy.

I. INTRODUCTION

This paper discusses and solves a new two-dimensional statistical mechanics problem called the pseudo-free 32 vertex model. It is a generalization of the free-fermion model, which, in turn, is a generalization of the Ising model (certain values of the parameters reproduce these two models). In addition, it includes several Ising-like models on various types of lattices as well as ferroelectric systems on the triangular lattice. This very general model involves eighteen parameters and yet it is exactly solvable. Section III computes the partition function. For Ising-like subcases, there is a simple way to calculate the vacuum expectation value of an arbitrary product of spins. An example is illustrated in Sec. VI.

This paper is a computational one. It uses integrals over anticommuting variables. The techniques were developed in two previous papers[1,2]. They were pedagogical in nature and formed the basis for this work. I recommend the study of these two papers for those readers interested in understanding the methods of this paper.

Paper I reviewed integrals over anticommuting variables and showed how they could be applied to statistical mechanics problems. In general, what resulted was an integral over an action, or equivalently a fermionic-like field theory. Several models had quadratic actions such as the Ising model. These models were called pseudo-free and were exactly solvable. This is why the Ising model is solvable; it is a fermionic free field theory. Paper II stressed calculational techniques. The partition function of several models were evaluated in II. Graphical methods and a set of computational rules were obtained. This allowed one to quickly solve the solvable (quadratic action) models. In general, the evaluation of a partion function was reduced to solving a miniature dimer problem (MDP). Using this, general rules were derived for solving a class of two dimensional close-packed dimer problems. Finally, paper II reduced the calculation of anticommuting variable correlation functions to solving modified miniature dimer problems (MMDP's). For Ising-like cases, these results can be used to calculate the vacuum expectation value of any product of spin variables.

Papers I and II dealt with models previously solved by other means. They formed the testing ground to see how the methods worked. This paper solves a new model never before considered. Papers I and II have stressed the importance of finding exactly solvable models as a first step for approaching unsolved models.

The 32 vertex model is quite complicated, having 18 free parameters. The partition function involves calculating 265 terms and the anticommuting variable correlation calculations have over 1000 terms, however simplifying tricks are used. Without these, the problem would be too tedious to solve. Furthermore, the results could not be presented in publishable form because equations would be too long. The anticommuting variables allow systematic evaluation and compactification of algebra. This causes roughly a seven-fold reduction in algebra. Computationally, the anticommuting variables are powerful objects.

Section II introduces the model. The anticommuting variable action is given in Eqs. (2.1) - (2.5). The 32 different configurations and their weights are shown in table 1.

Section III calculates the partition function. Its value is given in Eq. (3.6). The key function is L which is the determinant in Eqs. (3.4) and (3.5). The rest of the section is devoted to explicitly calculating L . Equation (3.31) writes L as a sum of three other functions, L^1, L^2, and L^3. Equations (3.8), (3.13), and (3.30) give L^1, L^2, and L^3.

Section IV and V evaluate the anticommuting variable correlations in momentum space and coordinate space. These results are presented in Eqs. (4.9) - (4.30) and Eqs. (5.1) - (5.21). This second set of equations is useful for solving problems related to the pseudo-free 32 vertex model. Section VI uses them to calculate the correlation function of two vertical spins in the triangular Ising model.

II. THE MODEL

The two-dimensional Ising model is equivalent to the partition function of closed polygons[3] where sides may intersect but cannot overlap. There is a Boltzmann factor per unit length of side. The Ising model is not the most general easily solvable model. The corners of polygons may also be weighted, resulting in the so-called free-fermion model[4,5] described by the action of Eq. (I.4.4) whose weights are given in Fig. I. 11. Let $w_{(p)}$ be the weight of Figs. I. 11P. Then, the following constraint, known as the free-fermion constraint, is satisfied:

$$w_{(a)}w_{(h)} + w_{(b)}w_{(c)} = w_{(d)}w_{(f)} + w_{(e)}w_{(g)} \quad (2.1)$$

Because of Eq. (2.1) the free-fermion model is not the most general eight-vertex model, although it is the most general easily solvable model.

Slightly more complicated than the basic Ising model would be to include next nearest neighbor interactions. Consider adding one set of diagonal interactions. Using bond variables leads to the closed polygon partition function drawn on the lattice of Fig. 1a. In the same sense that the free-fermion model is the solvable generalization of the square lattice Ising model, the pseudo-free 32 vertex model is the generalization of the triangular lattice (Fig. 1b) Ising model. The corners are weighted in addition to the sides. In short, the 32 vertex model is the partition function for closed polygons drawn on the lattice of Fig. 1a where sides and corners are weighted. This model contains many others: Mentioned already are the square and triangular lattice Ising models. In addition, duality enables the Ising model on the hexangonal lattice of Fig. 1c to be included. By setting diagonal couplings equal to zero, the usual free-fermion model is obtained.

Such a general model is, indeed, complicated. It involves 18 parameters (the simpler free-fermion model has 8). The phase diagram will be more complicated since it is an 18 dimensional space, and will have an interesting set of phase transitions and critical phenomenon. None of these topics, however, is analyzed in this paper. For a model of interest or for a given choice of parameters, the thermodynamics of the system is determined by the partition function [Eq. (3.6)] or the free energy per unit site [Eq. (3.7)]. Taking temperature derivatives will yield the energy and specific heat.

In I and II anticommuting variables were used to draw polygons on a square lattice. This lead to a Grassmann integral over a quadratic action, an exactly solvable fermionic-like pseudo-free

field theory. The action consisted of three pieces: a Bloch wall piece, a corner piece, and a monomer piece. The Bloch wall action drew the walls, the corner action formed the corners, and the monomer piece filled in all unfilled sites. Likewise, in dealing with polygons on the lattice of Fig. 1a, three terms are needed:

$$A_{32} = A_{\text{wall}} + A_{\text{corners}} + A_{\text{monomers}} \quad (2.2)$$

$$A_{\text{wall}} = \sum_{\alpha\beta} \left(z_h \eta^{h\dagger}_{\alpha\beta}\eta^{h}_{\alpha+1\beta} + z_v \eta^{v\dagger}_{\alpha\beta}\eta^{v}_{\alpha\beta+1} + z_d \eta^{d\dagger}_{\alpha\beta}\eta^{d}_{\alpha+1\ \beta+1} \right) . \quad (2.3)$$

$$\begin{aligned} A_{\text{corners}} = \sum_{\alpha\beta} \Big[& a_1 \eta^{h\dagger}_{\alpha\beta}\eta^{v}_{\alpha\beta} + a_2 \eta^{v\dagger}_{\alpha\beta}\eta^{h\dagger}_{\alpha\beta} + a_3 \eta^{v\dagger}_{\alpha\beta}\eta^{h}_{\alpha\beta} + a_4 \eta^{v}_{\alpha\beta}\eta^{h}_{\alpha\beta} \\ & + b_1 \eta^{d\dagger}_{\alpha\beta}\eta^{v}_{\alpha\beta} + b_2 \eta^{v\dagger}_{\alpha\beta}\eta^{d\dagger}_{\alpha\beta} + b_3 \eta^{v\dagger}_{\alpha\beta}\eta^{d}_{\alpha\beta} + b_4 \eta^{v}_{\alpha\beta}\eta^{d}_{\alpha\beta} \quad (2.4) \\ & + c_1 \eta^{h\dagger}_{\alpha\beta}\eta^{d}_{\alpha\beta} + c_2 \eta^{d\dagger}_{\alpha\beta}\eta^{h\dagger}_{\alpha\beta} + c_3 \eta^{d\dagger}_{\alpha\beta}\eta^{h}_{\alpha\beta} + c_4 \eta^{d}_{\alpha\beta}\eta^{h}_{\alpha\beta} \Big] . \end{aligned}$$

$$A_{\text{monomer}} = \sum_{\alpha\beta} \left[b_h \eta^{h}_{\alpha\beta}\eta^{h\dagger}_{\alpha\beta} + b_v \eta^{v}_{\alpha\beta}\eta^{v\dagger}_{\alpha\beta} + b_d \eta^{d}_{\alpha\beta}\eta^{d\dagger}_{\alpha\beta} \right] . \quad (2.5)$$

Three types (horizontal, vertical, and diagonal) of anticommuting variables are used at each site denoted by the superscripts, "h", "v", and "d". The subscripts "α" and "β" label the lattice sites and take on integer values. They are respectively the x and y coordinates of a site. The variables z_h, z_v, and z_d are the horizontal, vertical, and diagonal Boltzmann factors. The a's, b's, and c's are just constants. Each term in Eq. (2.3) and Eq. (2.4) has the graphical representation of Fig. 2 and Fig. 3. As in I and II, the following conventions are used: Arrows indicate the order of variables, "o"'s and "x"'s respectively refer to undaggered and daggered variables, and a horizontal, vertical, or diagonal line attached to a variable indicates whether it is a horizontal, vertical, or diagonal type.

There are 32 possible vertex configurations. These are shown in table 1. It is straightforward to calculate their weights using the action of Eq. (2.2). These are also given in table 1 with Bloch wall Boltzmann factors extracted. No minus signs result from reordering of anticommuting variables for non self-intersecting polygons. This can be proven by induction on the area of a polygon[6]. When lines intersect, however, a minus sign does result from reorderings. This is because of "fermi statistics" and is discussed in I. A few examples are shown in Fig. 4. This accounts for the extra minus signs in boxes (xvii), (xviii), (xix), (xxi), (xxiii), (xxiv), (xxvi), (xxviii), (xxx), and (xxxii) of table 1. In calculating the weights of boxes (v) through (xvi), one must be careful to include the possibility of two corners forming a third. For example, in box (v) an a_1 corner and a diagonal monomer could be used, but, for example, a c_1 corner followed by a b_1 corner can also be used, in which case all variables at the site are used up and no monomers are needed. The weight is $b_1 c_1$. Likewise a c_2 corner followed by a b_4 corner may be used. This accounts for all the weight factors in box (v). In calculating the weights of configurations (i) through (iv) one must be careful to include the

possibility that two corners can "act like" two monomers. For example, in box (iii) all horizontal and vertical sites must get filled. Although this could be done using the vertical and horizontal monomers, the corners a_1 and a_3 or a_2 and a_4 also combine to fill up the unoccupied sites.

Equations (2.2) - (2.5) and table 1 summarize the results for the pseudo-free 32 vertex model.

When

$$a_1 = a_3 = b_2 = b_4 = c_2 = c_4 = -1 ,$$

$$b_v = b_h = b_d = a_2 = a_4 = b_1 = b_3 = c_1 = c_3 = +1 , \quad (2.6)$$

the weights of table 1 are all -1 . Thus, the closed polygon partition function on a triangular lattice with unit weights for corners is

$$Z_{\text{closed polygon}} = (-1)^N \int d\eta d\eta^\dagger \exp A , \quad (2.7)$$

with A given by Eq. (2.2) with the values of Eq. (2.6). The $(-1)^N$ (N is the total # of sites) makes the weights of table 1 positive. In calculating $Z_{\text{closed polygon}}$, sides of polygons may not overlap. The relation between the triangular Ising model and $Z_{\text{closed polygon}}$ is

$$Z_{\triangle\ \text{Ising}} = (2 \cosh \beta J_h \cosh \beta J_v \cosh \beta J_d)^N Z_{\text{closed polygon}}, \quad (2.8)$$

with

$$z_h = \tanh \beta J_h ,$$
$$z_v = \tanh \beta J_v , \quad (2.9)$$
$$z_d = \tanh \beta J_d .$$

The J's are the coupling strengths of the spin-spin interactions. Although the main interest of this paper is the general model, the known triangular Ising model results will be used as a check. The hexangonal lattice Ising model has a similar representation (one must use disorder variables) in terms of $Z_{\text{closed polygon}}$:

$$Z_{\text{hexangonal lattiec}} = [\exp(\beta J_h + \beta J_d + \beta J_{d'})]^N Z_{\text{closed polygon}}, \tag{2.10}$$

with

$$z_v = \exp(-2\beta J_h),$$
$$z_h = \exp(-2\beta J_d), \tag{2.11}$$
$$z_d = \exp(-2\beta J_{d'}).$$

The couplings J_h, J_d, and $J_{d'}$ are the horizontal and diagonal ones of the lattice of Fig. 1c.

III. EVALUATION OF THE PARTITION FUNCTION

The main results of this section are contained in Eqs. (3.4), (3.5) and (3.6).

The pseudo-free 32 vertex partition function is described by the action of Eq. (2.2). It is evaluated by going to momentum space. This partially diagonalizes the problem. The method is described in II. Formulas (II. 2.1) and (II. 2.3) are used. The result is an action in momentum variables of the form

$$\begin{aligned} A_{32} = \sum_{st}\Big[&\left(v_t a^v_{st} a^{v\dagger}_{st} + h_s a^h_{st} a^{h\dagger}_{st} + d_{st} a^d_{st} a^{d\dagger}_{st}\right) \\ &+ \left(a_1 a^{h\dagger}_{st} a^v_{st} + a_3 a^{v\dagger}_{st} a^h_{st} + a_2 a^{v\dagger}_{st} a^{h\dagger}_{-s-t} + a_4 a^v_{st} a^h_{-s-t}\right) \\ &+ \left(b_1 a^{d\dagger}_{st} a^v_{st} + b_3 a^{v\dagger}_{st} a^d_{st} + b_2 a^{v\dagger}_{st} a^{d\dagger}_{-s-t} + b_4 a^v_{st} a^d_{-s-t}\right) \\ &+ \left(c_1 a^{h\dagger}_{st} a^d_{st} + c_3 a^{d\dagger}_{st} a^h_{st} + c_2 a^{d\dagger}_{st} a^{h\dagger}_{-s-t} + c_4 a^d_{st} a^h_{-s-t}\right)\Big], \end{aligned} \tag{3.1}$$

where

$$\begin{aligned} v_t &= b_v - z_v \exp\left(\frac{2\pi i t}{2N+1}\right), \\ h_s &= b_h - z_h \exp\left(\frac{2\pi i s}{2M+1}\right), \\ d_{st} &= b_d - z_d \exp\left(\frac{2\pi i s}{2M+1} + \frac{2\pi i t}{2N+1}\right). \end{aligned} \tag{3.2}$$

The lattice has been taken to consist of $(2N+1)$ rows by $(2M+1)$ columns of sites. When the thermodynamic limit is taken, it is useful to use the momentum variables $p_x \equiv \frac{2\pi s}{2M+1}$ and $p_y = \frac{2\pi t}{2N+1}$ and the functions

$$\begin{aligned} v(p_y) &= b_v - z_v \exp(ip_y), \\ h(p_x) &= b_h - z_h \exp(ip_x), \\ d(p_x,p_y) &= b_d - z_d \exp(ip_x + ip_y). \end{aligned} \tag{3.3}$$

The graphical method (described in II) will be used. The result is the miniature dimer problem (MDP) of Fig. 5. This problem has twelve sites and thirty bonds. In order not to make the figure messy, four copies have been made in Fig. 5. Each copy contains a subset of bonds and displays their weights. For the total MDP, put all bonds on the same twelve sites. By transforming $a^{v}_{-s-t} \leftrightarrow a^{v^+}_{-s-t}$, $a^{h}_{-s-t} \leftrightarrow a^{h^+}_{-s-t}$, and $a^{d}_{-s-t} \leftrightarrow a^{d^+}_{-s-t}$, the problem becomes of aa^+ form. According to Eq. (I. 2.6), this is the determinant of the following matrix

$$M(p_x, p_y) = \begin{pmatrix} v(p_y) & -a_1 & -b_1 & 0 & a_4 & b_4 \\ -a_3 & h(p_x) & -c_3 & -a_4 & 0 & -c_4 \\ -b_3 & -c_1 & d(p_x,p_y) & -b_4 & c_4 & 0 \\ 0 & a_2 & b_2 & -v(-p_y) & a_3 & b_3 \\ -a_2 & 0 & -c_2 & a_1 & -h(-p_x) & c_1 \\ -b_2 & c_2 & 0 & b_1 & c_3 & -d(-p_x,-p_y) \end{pmatrix} . \qquad (3.4)$$

$$L(p_x, p_y) = \det M(p_x, p_y). \qquad (3.5)$$

In the thermodynamic limit, the answer is

$$Z_{32} = \exp\left\{ (2N + 1)(2M + 1) \frac{1}{2} \int_{-\pi}^{\pi} \frac{dp_x}{2\pi} \int_{-\pi}^{\pi} \frac{dp_y}{2\pi} \ell n\, L(p_x,p_y) \right\} . \qquad (3.6)$$

The free energy, f, per unit site is

$$-\beta f = \frac{1}{2} \int_{-\pi}^{\pi} \frac{dp_x}{2\pi} \int_{-\pi}^{\pi} \frac{dp_y}{2\,\pi} \ell n\, L(p_x,p_y) . \qquad (3.7)$$

A 6×6 determinant, in general, has 720 terms. The matrix, $M(p_x,p_y)$, however, has six zero entries, which reduces this number to 265. For particular values of the parameters a_i, b_i, c_i, etc. one may use computers to evaluate Eq. (3.5). For general values, all 265 terms must be evaluated. This will be done using the graphical method. A brute force application would find and calculate all 265 coverings of Fig. 5, a process which is tedious, not useful, and results in an answer too cumbersome to be published. I circumvent this by using the following device: If the bonds in Figs. 5c and 5d are removed, what remains is the free fermion model. In II, the partition function and correlation functions were calculated. These result may be used as a calculational foundation. There are three types of terms: type 1 are proportional to $d(p_x, p_y)d(-p_x,-p_y)$, type 2 involve either $d(p_x, p_y)$ or $d(-p_x, -p_y)$, and type 3 involve neither $d(p_x, p_y)$ nor $d(-p_x,-p_y)$ and must use four bonds from Figs. 5c and 5d. Each of the three types will be systematically evaluated using results from II.

Type 1. After the $d(p_x, p_y)$ and $d(-p_x,-p_y)$ bonds have been used, what remains is the free fermion MDP whose value was given in Eq. (II. 3.3). The contribution of type 1 is

$$L^1(p_x, p_y) = d(p_x, p_y)d(-p_x, -p_y)L_{f.f.}(p_x, p_y), \qquad (3.8)$$

where

$$L_{f.f}(p_x,p_y) = h(p_x)h(-p_x)v(p_y)v(-p_y) - a_1a_3[h(p_x)v(p_y) + h(-p_x)v(-p_y)]$$

$$- a_2a_4[h(p_x)v(-p_y) + h(-p_x)v(p_y)] + (a_1a_3 + a_2a_4)^2 \; . \qquad (3.9)$$

Nine of the 265 terms are contained in L^1.

Type 2. These terms are proportional to $d(p_x, p_y)$ or $d(-p_x,-p_y)$. They must use two bonds from Figs. 5c and 5d. When $d(-p_x, -p_y)$ is used, the diagonal (s, t) sites must be covered by one bond from Figure 5c, say b_1, and one from Fig. 5d, say b_3 (see table 2, box 1 above A_1). What results is the modified miniature dimer problem (MMDP) used in calculating the correlation $\langle a^v_{st}a^{v+}_{st}\rangle$ of the free-fermion model. The value of the MMDP, $W_1(p_x, p_y)$, is given in Eq. (II. 5.3). There is another way in which this MMDP can occur using $d(p_x, p_y)$ and the b_4 and b_2 bonds connecting to diagonal $(-s, -t)$ sites (see table 2, box 1 above B_1). Summing these two terms yields

$$W_1(p_x, p_y)[d(-p_x, -p_y)(-b_1b_3) + d(p_x, p_y)(-b_2b_4)] \; , \qquad (3.10)$$

and, in general, yields schematically

(weight of MMDP)[$d(-p_x, -p_y)$(bond weight for (s,t) diagonal variables

+ $d(p_x, p_y)$(bond weights for $(-s, -t)$ diagonal variables)]. (3.11)

The sign of the bond weights is determined using the sign rules (a) and (b) of Fig. I.8.

All together there are 16 possible MMDP's. These are shown in table 2, column 1. Let $W_i(p_x, p_y)$ be the values of the coverings. The W_i were obtained from Figs. II. 21 - II. 32 and Eqs. (II. 5.2) - (II. 5.17) and are listed below. Let A_i and B_i be the values of bond weights for (s, t) and $(-s, -t)$ diagonal sites. The numbers, A_i and B_i, are given in colums 2 and 3 of table 2. Let

$$C_i(p_x, p_y) \equiv [d(-p_x, -p_y)A_i + d(p_x, p_y)B_i]. \qquad (3.12)$$

then

$$L^2(p_x, p_y) = \sum_{i=1}^{16} W_i(p_x, p_y)C_i(p_x, p_y) \; . \qquad (3.13)$$

For completeness the $W_i(p_x, p_y)$ are given:

$$W_1(p_x, p_y) = h(p_x)h(-p_x)v(-p_y) - a_1a_3h(p_x) - a_2a_4h(-p_x), \qquad (3.14)$$

$$W_2(p_x, p_y) = W_1(-p_x,-p_y), \qquad (3.15)$$

$$W_3(p_x, p_y) = h(-p_x)v(p_y)v(-p_y) - a_1a_3v(p_y) - a_2a_4v(-p_y), \qquad (3.16)$$

$$W_4(p_x, p_y) = W_3(-p_x,-p_y), \qquad (3.17)$$

$$W_5(p_x, p_y) = a_3[(a_1a_3 + a_2a_4) - h(-p_x)v(-p_y)], \qquad (3.18)$$

$$W_6(p_x, p_y) = W_5(-p_x, -p_y), \qquad (3.19)$$

$$W_7(p_x, p_y) = a_1[(a_1a_3 + a_2a_4) - h(-p_x)v(-p_y)] \qquad (3.20)$$

$$W_8(p_x, p_y) = W_7(-p_x, -p_y), \qquad (3.21)$$

$$W_9(p_x, p_y) = a_4[(a_1a_3 + a_2a_4) - h(p_x)v(-p_y)], \quad (3.22)$$

$$W_{10}(p_x, p_y) = W_9(-p_x, -p_y), \quad (3.23)$$

$$W_{11}(p_x, p_y) = a_2[(a_1a_3 + a_2a_4) - h(p_x)v(-p_y)], \quad (3.24)$$

$$W_{12}(p_x, p_y) = W_{11}(-p_x, -p_y), \quad (3.25)$$

$$W_{13}(p_x, p_y) = a_1a_4[h(-p_x) - h(p_x)], \quad (3.26)$$

$$W_{14}(p_x, p_y) = a_2a_3[h(-p_x) - h(p_x)], \quad (3.27)$$

$$W_{15}(p_x, p_y) = a_3a_4[v(p_y) - v(-p_y)], \quad (3.28)$$

$$W_{16}(p_x, p_y) = a_1a_2[v(p_y) - v(-p_y)] \,. \quad (3.29)$$

Eighty-eight of the 265 terms are in L^2 .

Type 3. These terms involve two bonds from Fig. 5c and two bonds from Fig. 5d and cover four sites in the free-fermion model (see the first column of table 3). The uncovered sites form an MMDP whose covering(s) is shown in the second column of table 3 and whose value is called F_i. Let E_i be the value of bonds of Figs. 5c and 5d which go in forming the MMDP. The value of a diagram is E_iF_i. Therefore,

$$L^3(p_x, p_y) = \sum_{i=1}^{36} E_iF_i(p_x, p_y). \quad (3.30)$$

The E_i and F_i values are given in table 3. Boxes 1 - 6 of table 3 have 40 terms, boxes 7 - 12 have 32 terms, and boxes 13 - 36 have 96 terms. Thus, L^3 contains the remaining 168 terms.

The final result is

$$L(p_x, p_y) = L^1(p_x, p_y) + L^2(p_x, p_y) + L^3(p_x, p_y), \quad (3.31)$$

where L^1, L^2, and L^3 are given in Eqs. (3.8), (3.13), and (3.30).

Although a lot of algebra has gone into evaluating $L(p_x, p_y)$, it is justified, since the next section reuses this algebra.

Of interest are the values for the triangular Ising model [Eqs. (2.6) - (2.9)]:

$$\begin{aligned} v(p_y) &= 1 - z_v \exp(ip_y), \\ h(p_x) &= 1 - z_h \exp(ip_x), \\ d(p_x, p_y) &= 1 - z_d \exp(ip_x + ip_y). \end{aligned} \quad (3.32)$$

$$\begin{aligned} &A_1 = A_2 = A_3 = A_4 = A_6 = A_8 = A_9 = A_{10} = A_{11} = A_{12} = A_{15} = A_{16} = -1, \\ &A_5 = A_7 = A_{13} = A_{14} = 1 \,, \\ &B_1 = B_2 = B_3 = B_4 = B_5 = B_7 = B_9 = B_{10} = B_{11} = B_{12} = B_{13} = B_{14} = -1, \\ &B_6 = B_8 = B_{15} = B_{16} = 1 \,. \end{aligned} \quad (3.33)$$

$$\begin{aligned} &C_1 = C_2 = C_3 = C_4 = C_9 = C_{10} = C_{11} = C_{12} = -2 + 2z_d \cos(p_x + p_y) \,, \\ &C_5 = -C_6 = C_7 = -C_8 = C_{13} = C_{14} = -C_{15} = -C_{16} = 2z_d \, i \sin(p_x + p_y). \end{aligned} \quad (3.34)$$

$$W_1(p_x,p_y) = W_2(-p_x,-p_y) = \left[-1 + z_h^2 - (1 + z_h^2 - 2z_h \cos p_x) z_v \exp(-ip_y)\right] ,$$

$$W_3(p_x,p_y) = W_4(-p_x,-p_y) = \left[-1 + z_v^2 - (1 + z_v^2 - 2z_v \cos p_y) z_h \exp(-ip_x)\right] ,$$

$$W_5(p_x,p_y) = W_6(-p_x,-p_y) = W_7(p_x,p_y) = W_8(-p_x,-p_y) = - W_9(-p_x,p_y)$$

$$= - W_{10}(p_x,-p_y) = - W_{11}(-p_x,p_y) = - W_{12}(p_x,-p_y) \qquad (3.35)$$

$$= \left[- 1 - z_h \exp(-ip_x) - z_v \exp(-ip_y) + z_v z_h \exp(-ip_x - ip_y) \right] ,$$

$$W_{13}(p_x) = W_{14}(p_x) = - 2iz_h \sin p_x ,$$

$$W_{15}(p_y) = W_{16}(p_y) = 2iz_v \sin p_y .$$

The non-zero E_i are

$$E_1 = E_2 = E_5 = E_6 = E_8 = E_9 = E_{11} = E_{12} = E_{15} = E_{16} =$$
$$= E_{21} = E_{22} = E_{27} = E_{28} = E_{33} = E_{34} = 4. \qquad (3.36)$$

$$F_1(p_x) = 1 + z_h^2 - 2z_h \cos p_x ,$$

$$F_2(p_x,p_y) = F_3(-p_x,p_y) = F_4(p_x,-p_y) = F_5(-p_x,-p_y)$$

$$= \left[- z_h \exp(-ip_x) - z_v \exp(-ip_y) + z_v z_h \exp(-ip_x - ip_y)\right] ,$$

$$F_6(p_y) = 1 + z_v^2 - 2z_v \cos p_y , \qquad (3.37)$$

$$F_7 = F_{10} = F_{11} = F_{12} = -F_{17} = -F_{18} = F_{23} = F_{24} = F_{29} = F_{30}$$

$$= - F_{35} = - F_{36} = 1,$$

$$F_8 = F_9 = 2,$$

$$F_{13}(p_x) = F_{14}(p_x) = - F_{15}(-p_x) = - F_{16}(-p_x) = F_{19}(-p_x) = F_{20}(-p_x)$$

$$= - F_{21}(p_x) = - F_{22}(p_x) = 1 - z_h \exp(ip_x) ,$$

$$F_{25}(p_y) = F_{26}(p_y) = - F_{27}(-p_y) = - F_{28}(-p_y) = F_{31}(-p_y) = F_{32}(-p_y)$$

$$= - F_{33}(p_y) = - F_{34}(p_y) = 1 - z_v \exp(ip_y).$$

$$L^1 = \left[1 + z_d^2 - 2z_d \cos(p_x + p_y)\right]\left[(1 + z_h^2)(1 + z_v^2) + 2(1 - z_v^2) z_h \cos p_x + 2(1 - z_h^2) z_v \cos p_y\right] ,$$

$$L^2 = \left\{4 \left[z_d \cos (p_x + p_y) - 1\right] \left[z_h^2 + z_v(1 - z_h^2) \cos p_y + z_v^2 + z_h(1 - z_v^2) \cos p_x\right] + 8z_v z_d z_h - 8z_v z_h \cos(p_x + p_y)\right\} \qquad (3.38)$$

$$L^3 = 4\left[z_h^2 + z_v^2 + 2z_v z_h \cos(p_x + p_y)\right] .$$

$$L = \Big\{ (1 + z_d^2)(1 + z_h^2)(1 + z_v^2) - 2(1 - z_d^2)(1 - z_v^2) z_h \cos p_x$$
$$- 2(1 - z_d^2)(1 - z_h^2) z_v \cos p_y - 2(1 - z_h^2)(1 - z_v^2) z_d \cos(p_x + p_y)$$
$$+ 8z_d z_v z_h \Big\} . \qquad (3.39)$$

The free energy per unit site, $f_\triangle$, for the triangular Ising model (or rectangular Ising model with one diagonal interaction) is

$$-\beta f_{\triangle} = \frac{1}{2}\int_{-\pi}^{\pi}\frac{dp_x}{2\pi}\int_{-\pi}^{\pi}\frac{dp_y}{2\pi}\,\ell n\left[(2\cosh\,\beta J_h\cosh\,\beta J_v\cosh\,\beta J_d)^2 L(p_x,p_y)\right] . \qquad (3.40)$$

This agrees with the known answer[7].

IV. THE MOMENTUM SPACE CORRELATIONS

This section calculates the momentum space anticommuting variable correlation functions using the graphical methods developed in II. This becomes equivalent to solving modified miniature dimer problems (MMDP's). There are 21 non-zero different correlations (15 are zero). Each involves a large number of coverings (approximately 50). If brute force methods are used, a total of roughly 1000 coverings must be found and their corresponding weights calculated. Such a process would be tedious. Fortunately, symmetry properties of the pseudo-free 32 vertex MDP determine 15 of the non-zero correlations in terms of 6. Furthermore, the results of Sec. III eliminate the need to find the 50 coverings. Instead, less than 20 terms must be found. All in all, roughly 1000 calculations are reduced to a little more than 100. This is fortunate since without these tricks the correlations could not be presented in a compact or readable form.

I will describe in detail how $\langle a^v_{st} a^{v\dagger}_{st}\rangle$ is calculated. The results for the remaining five correlations will then be simply stated. Finally, symmetry properties will be used to obtain the remaining ones. Momentum variables, p_x and p_y, will be used to express the answers.

To calculate $\langle a^v_{st} a^{v\dagger}_{st}\rangle$, insert the superbond shown in Fig. 6 and erase the bonds in Fig. 5 which connect to vertical (s,t) sites.

The resulting problem is the MMDP whose weight will be called V_1. Analogous to the partition function, three terms contribute to V_1: type 1, which are proportional to $d(p_x,p_y)d(-p_x, -p_y)$, type 2, which are proportional to either $d(p_x, p_y)$ or $d(-p_x,-p_y)$, and type 3, which involve neither $d(p_x,p_y)$ nor $d(-p_x, -p_y)$. Each will be evaluated in turn.

Type 1. After using the $d(p_x, p_y)$ and $d(-p_x, -p_y)$ bonds, the diagonal sites are exhausted. What remains is the free fermion expectation $\langle a^v_{st} a^{v\dagger}_{st}\rangle_{ff} = W_1(p_x, p_y)$. Therefore type 1 contributes

$$W_1(p_x, p_y)d(p_x, p_y)d(-p_x, -p_y). \qquad (4.1)$$

This is symbolically displayed in Fig. 7.

Type 2. These involve either $d(p_x, p_y)$ or $d(-p_x, -p_y)$. The other diagonal "o" and "x" must be covered by bonds of Figs. 5c or 5d or alternatively those of table 2. Only bonds which do not connect to vertical (s,t) sites may be used. These are those in boxes 2,3,4,6,8,10,12,15 and 16 of table 2. Consider box 2. When $d(p_x, p_y)$ is used, B_2 bonds must be used and when $d(-p_x, -p_y)$ is used, A_2 bonds must be used. This results in the factor $C_2 = d(-p_x, -p_y)A_2 + d(p_x, p_y)B_2$. In either case the resulting diagram is Fig. 8a which is an MMDP with two superbonds. Its covering is in the second column of box 1 in table 3. The weight is F_1. The contribution is, therefore, C_2F_1. The nine different type 2 terms along with their weights are shown in Fig. 8. Their total contribution is

$$C_2F_1 + C_3F_2 + C_4F_3 + C_6F_{13} + C_8F_{14} + C_{10}F_{15} + C_{12}F_{16} + C_{15}F_{17} + C_{16}F_{18}. \qquad (4.2)$$

Type 3. These involve four bonds from Figs. 5c and 5d. They will cover up four h and v sites besides the two vertical (s, t) ones. These sites could be those in boxes 4, 5, 6, 23, 24; 25, 26, 33, and 34 of table 3. If box 4 sites were used, there would be four ways of doing this, the sum of which results in the factor E_4. What remains is the MMDP of Fig. 9a which has 3 superbonds. Its covering is $h(-p_x)$. Box 4 contributes $E_4h(-p_x)$. Figure 9 shows the nine type 3 diagrams and their contributions. They sum to

$$E_4h(-p_x) + E_5h(p_x) + E_6v(-p_y) - E_{25}a_3 - E_{26}a_1 - E_{33}a_4 - E_{34}a_2 \quad (4.3)$$

The sum of Equ. (4.1), (4.2), and (4.3) is V_1, which is given in box 1 of table 4.

Let V_i be the weights of the MMDP's associated with correlations in the i^{th} box of table 4. V_1, V_7, V_{19}, V_{25}, V_{31}, and V_{32} were calculated using the method illustrated for V_1. The remaining ones are obtained by using transformations (i.e. symmetries) of the MDP of Fig. 5 Consider Fig. 5. Suppose horizontal and vertical sites are interchanged. What results is the same MDP except that bond weights get redefined. For a horizontal-vertical transformation one finds:

<u>Transformation (i) Vertical ↔ Horizontal.</u>

$$\begin{array}{ll} a_1 \leftrightarrow a_3, & b_4 \leftrightarrow -c_4, \\ a_2 \rightarrow -a_2, & v \leftrightarrow h\ . \\ a_4 \rightarrow -a_4, & \\ b_1 \leftrightarrow c_3, & \\ b_2 \leftrightarrow -c_2, & \\ b_3 \leftrightarrow c_1, & \end{array} \quad (4.4)$$

In Eq. (4.4) $v \leftrightarrow h$ stands for both $v(p_y) \leftrightarrow h(p_x)$ and $h(-p_x) \leftrightarrow v(-p_y)$. This transformation can be performed when a superbond is present, so that the V_3 of box 3 of table 4 is obtained from the V_1 of box 1 by Eq. (4.4). In using these transformations all functional dependence on the a_i, b_i, c_i, v, h, and d must be made manifest.

In all, there are 5 different transformations. They are used to obtain the remaining V_i . The others are

<u>Transformation (ii) Horizontal ↔ Diagonal.</u>

$$\begin{array}{ll} a_i \leftrightarrow b_i, & i = 1, 2, 3, \text{ or } 4 \\ c_1 \leftrightarrow c_3, & \\ c_2 \rightarrow -c_2, & \\ c_4 \rightarrow -c_4, & \\ h \leftrightarrow d\ . & \end{array} \quad (4.5)$$

<u>Transformation (iii) Vertical ↔ Diagonal.</u>

$$\begin{array}{l} a_i \leftrightarrow c_i, \\ b_1 \leftrightarrow b_3, \\ b_2 \rightarrow -b_2, \\ b_4 \rightarrow -b_4, \\ v \leftrightarrow d\ . \end{array} \quad (4.6)$$

<u>Transformation (iv) Vertical → Horizontal → Diagonal → Vertical.</u>

$$\begin{array}{lll} a_1 \rightarrow c_3, & b_2 \rightarrow -a_2, & h \rightarrow d, \\ a_2 \rightarrow -c_2, & b_3 \rightarrow a_1, & d \rightarrow v. \\ a_3 \rightarrow c_1, & b_4 \rightarrow -a_4, & \\ a_4 \rightarrow -c_4, & c_i \rightarrow b_i, & \\ b_1 \rightarrow a_3, & v \rightarrow h, & \end{array} \quad (4.7)$$

Transformation (v) Horizontal → Vertical → Diagonal → Horizontal.

$$\begin{aligned} a_1 &\to b_3, \\ a_2 &\to -b_2, \\ a_3 &\to b_1, \\ a_4 &\to -b_4, \\ b_i &\to c_i, \\ c_1 &\to a_3, \\ c_2 &\to -a_2, \\ c_3 &\to a_1, \\ c_4 &\to -a_4, \\ h &\to v, \\ v &\to d, \\ d &\to h. \end{aligned} \tag{4.8}$$

For $i \leqslant 15$, define $V_{2i}(p_x, p_y) = V_{2i-1}(-p_x, -p_y)$. The V_i are the pseudo-free 32 vertex analogues of the free-fermion W_i.

The results for the momentum space correlations are

$$\langle a^v_{st} a^{v\dagger}_{st} \rangle = V_1(p_x, p_y) \; / \; L(p_x, p_y). \tag{4.9}$$

$$\langle a^h_{st} a^{h\dagger}_{st} \rangle = V_3(p_x, p_y) \; / \; L(p_x, p_y). \tag{4.10}$$

$$\langle a^d_{st} a^{d\dagger}_{st} \rangle = V_5(p_x, p_y) \; / \; L(p_x, p_y). \tag{4.11}$$

$$\langle a^{h\dagger}_{st} a^v_{st} \rangle = V_7(p_x, p_y) \; / \; L(p_x, p_y). \tag{4.12}$$

$$\langle a^{d\dagger}_{st} a^v_{st} \rangle = V_9(p_x, p_y) \; / \; L(p_x, p_y). \tag{4.13}$$

$$\langle a^{d\dagger}_{st} a^h_{st} \rangle = V_{11}(p_x, p_y) \; / \; L(p_x, p_y). \tag{4.14}$$

$$\langle a^{v\dagger}_{st} a^h_{st} \rangle = V_{13}(p_x, p_y) \; / \; L(p_x, p_y). \tag{4.15}$$

$$\langle a^{v\dagger}_{st} a^d_{st} \rangle = V_{15}(p_x, p_y) \; / \; L(p_x, p_y). \tag{4.16}$$

$$\langle a^{h\dagger}_{st} a^d_{st} \rangle = V_{17}(p_x, p_y) \; / \; L(p_x, p_y). \tag{4.17}$$

$$\langle a^{v\dagger}_{st} a^{h\dagger}_{-s-t} \rangle = V_{19}(p_x, p_y) \; / \; L(p_x, p_y). \tag{4.18}$$

$$\langle a^{v\dagger}_{st} a^{d\dagger}_{-s-t} \rangle = V_{21}(p_x, p_y) \; / \; L(p_x, p_y). \tag{4.19}$$

$$\langle a^{h\dagger}_{st} a^{d\dagger}_{-s-t} \rangle = V_{23}(p_x, p_y) \; / \; L(p_x, p_y). \tag{4.20}$$

$$\langle a^v_{st} a^h_{-s-t} \rangle = V_{25}(p_x, p_y) \; / \; L(p_x, p_y). \tag{4.21}$$

$$\langle a^v_{st} a^d_{-s-t} \rangle = V_{27}(p_x, p_y) \; / \; L(p_x, p_y). \tag{4.22}$$

$$\langle a^h_{st} a^d_{-s-t} \rangle = V_{29}(p_x, p_y) \; / \; L(p_x, p_y). \tag{4.23}$$

$$\langle a^{v\dagger}_{st} a^{v\dagger}_{-s-t} \rangle = V_{31}(p_x, p_y) \; / \; L(p_x, p_y). \tag{4.24}$$

$$\langle a^v_{st} a^v_{-s-t} \rangle = V_{32}(p_x, p_y) \; / \; L(p_x, p_y). \tag{4.25}$$

$$\langle a^{h\dagger}_{st} a^{h\dagger}_{-s-t} \rangle = V_{33}(p_x, p_y) \; / \; L(p_x, p_y). \tag{4.26}$$

$$\langle a^h_{st} a^h_{-s-t} \rangle = V_{34}(p_x, p_y) \; / \; L(p_x, p_y). \tag{4.27}$$

$$\langle a^{d\dagger}_{st} a^{d\dagger}_{-s-t} \rangle = V_{35}(p_x, p_y) \; / \; L(p_x, p_y). \tag{4.28}$$

$$\langle a^d_{st} a^d_{-s-t} \rangle = V_{36}(p_x, p_y) \; / \; L(p_x, p_y). \tag{4.29}$$

The zero correlations are

$$\langle a^{v\dagger}_{st} a^{h\dagger}_{st} \rangle = \langle a^{v}_{st} a^{h}_{st} \rangle = \langle a^{v\dagger}_{st} a^{d\dagger}_{st} \rangle = \langle a^{v}_{st} a^{d}_{st} \rangle =$$

$$\langle a^{h\dagger}_{st} a^{d\dagger}_{st} \rangle = \langle a^{h}_{st} a^{d}_{st} \rangle = \langle a^{v}_{st} a^{v\dagger}_{-s-t} \rangle = \langle a^{v}_{st} a^{h\dagger}_{-s-t} \rangle =$$

$$\langle a^{v}_{st} a^{d\dagger}_{-s-t} \rangle = \langle a^{h}_{st} a^{v\dagger}_{-s-t} \rangle = \langle a^{h}_{st} a^{h\dagger}_{-s-t} \rangle = \langle a^{h}_{st} a^{d\dagger}_{-s-t} \rangle = \qquad (4.30)$$

$$\langle a^{d}_{st} a^{v\dagger}_{-s-t} \rangle = \langle a^{d}_{st} a^{h\dagger}_{-s-t} \rangle = \langle a^{d}_{st} a^{d\dagger}_{-s-t} \rangle = 0 \ .$$

In Eqs. (4.9)-(4.30), $p_x = \frac{2\pi s}{2M+1}$ and $p_y = \frac{2\pi t}{2N+1}$. Equation (3.5) or (3.31) give $L(p_x, p_y)$ and the V_i are given in table 4. The correlations in Eq. (4.30) are zero. This can be seen immediately by interchanging "x"'s and "o"'s at (-s, -t) sites of the MDP of Fig.5. After doing this correlations are zero unless the number of "o"'s equals the number of "x"'s ("fermion number conservation").

V. THE COORDINATE SPACE CORRELATIONS

The coordinate space anticommuting variable correlation functions can be related to the momentum space ones of Eqs. (4.9)-(4.30) using Eq. (II. 2.3):

$$\langle \eta^{v}_{\alpha\beta} \eta^{v\dagger}_{\alpha'\beta'} \rangle = \int_{-\pi}^{\pi} \frac{dp_x}{2\pi} \int_{-\pi}^{\pi} \frac{dp_y}{2\pi} \exp[i(\alpha - \alpha')p_x + i(\beta - \beta')p_y] \times V_1(p_x, p_y) / L(p_x, p_y). \qquad (5.1)$$

$$\langle \eta^{h}_{\alpha\beta} \eta^{h\dagger}_{\alpha'\beta'} \rangle = \int_{-\pi}^{\pi} \frac{dp_x}{2\pi} \int_{-\pi}^{\pi} \frac{dp_y}{2\pi} \exp[i(\alpha - \alpha')p_x + i(\beta - \beta')p_y] \times V_3(p_x, p_y) / L(p_x, p_y). \qquad (5.2)$$

$$\langle \eta^{d}_{\alpha\beta} \eta^{d\dagger}_{\alpha'\beta'} \rangle = \int_{-\pi}^{\pi} \frac{dp_x}{2\pi} \int_{-\pi}^{\pi} \frac{dp_y}{2\pi} \exp[i(\alpha - \alpha')p_x + i(\beta - \beta')p_y] \times V_5(p_x, p_y) / L(p_x, p_y). \qquad (5.3)$$

$$\langle \eta^{v}_{\alpha\beta} \eta^{h\dagger}_{\alpha'\beta'} \rangle = -\int_{-\pi}^{\pi} \frac{dp_x}{2\pi} \int_{-\pi}^{\pi} \frac{dp_y}{2\pi} \exp[i(\alpha - \alpha')p_x + i(\beta - \beta')p_y] \times V_7(p_x, p_y) / L(p_x, p_y) . \qquad (5.4)$$

$$\langle \eta^{v}_{\alpha\beta} \eta^{d\dagger}_{\alpha'\beta'} \rangle = -\int_{-\pi}^{\pi} \frac{dp_x}{2\pi} \int_{-\pi}^{\pi} \frac{dp_y}{2\pi} \exp[i(\alpha - \alpha')p_x + i(\beta - \beta')p_y] \times V_9(p_x, p_y) / L(p_x, p_y). \qquad (5.5)$$

$$\langle \eta^{h}_{\alpha\beta} \eta^{d\dagger}_{\alpha'\beta'} \rangle = -\int_{-\pi}^{\pi} \frac{dp_x}{2\pi} \int_{-\pi}^{\pi} \frac{dp_x}{2\pi} \exp[i(\alpha - \alpha')p_x + i(\beta - \beta')p_y] \times V_{11}(p_x, p_y) / L(p_x, p_y) . \qquad (5.6)$$

$$\langle \eta^{h}_{\alpha\beta} \eta^{v\dagger}_{\alpha'\beta'} \rangle = -\int_{-\pi}^{\pi} \frac{dp_x}{2\pi} \int_{-\pi}^{\pi} \frac{dp_y}{2\pi} \exp[i(\alpha - \alpha')p_x + i(\beta - \beta')p_y] \times V_{13}(p_x, p_y) / L(p_x, p_y). \qquad (5.7)$$

$$\langle \eta^{d}_{\alpha\beta} \eta^{v\dagger}_{\alpha'\beta'} \rangle = -\int_{-\pi}^{\pi} \frac{dp_x}{2\pi} \int_{-\pi}^{\pi} \frac{dp_y}{2\pi} \exp[i(\alpha - \alpha')p_x + i(\beta - \beta')p_y] \times V_{15}(p_x, p_y) / L(p_x, p_y). \qquad (5.8)$$

$$\langle \eta^{d}_{\alpha\beta} \eta^{h\dagger}_{\alpha'\beta'} \rangle = -\int_{-\pi}^{\pi} \frac{dp_x}{2\pi} \int_{-\pi}^{\pi} \frac{dp_y}{2\pi} \exp[i(\alpha - \alpha')p_x + i(\beta - \beta')p_y] \times V_{17}(p_x, p_y) / L(p_x, p_y). \qquad (5.9)$$

$$\langle \eta^{v\dagger}_{\alpha\beta}\eta^{h\dagger}_{\alpha'\beta'}\rangle = \int_{-\pi}^{\pi} \frac{dp_x}{2\pi} \int_{-\pi}^{\pi} \frac{dp_y}{2\pi} \exp\,[i(\alpha' - \alpha)p_x + i(\beta' - \beta)p_y]$$

$$\times V_{19}(p_x, p_y) \,/\, L(p_x, p_y). \quad (5.10)$$

$$\langle \eta^{v\dagger}_{\alpha\beta}\eta^{d\dagger}_{\alpha'\beta'}\rangle = \int_{-\pi}^{\pi} \frac{dp_x}{2\pi} \int_{-\pi}^{\pi} \frac{dp_y}{2\pi} \exp\,[i(\alpha' - \alpha)p_x + i(\beta' - \beta)p_y]$$

$$\times V_{21}(p_x, p_y) \,/\, L(p_x, p_y). \quad (5.11)$$

$$\langle \eta^{h\dagger}_{\alpha\beta}\eta^{d\dagger}_{\alpha'\beta'}\rangle = \int_{-\pi}^{\pi} \frac{dp_x}{2\pi} \int_{-\pi}^{\pi} \frac{dp_y}{2\pi} \exp\,[i(\alpha' - \alpha)p_x + i(\beta' - \beta)p_y]$$

$$\times V_{23}(p_x, p_y) \,/\, L(p_x, p_y). \quad (5.12)$$

$$\langle \eta^{v}_{\alpha\beta}\eta^{h}_{\alpha'\beta'}\rangle = \int_{-\pi}^{\pi} \frac{dp_x}{2\pi} \int_{-\pi}^{\pi} \frac{dp_y}{2\pi} \exp\,[i(\alpha - \alpha')p_x + i(\beta - \beta')p_y]$$

$$\times V_{25}(p_x, p_y) \,/\, L(p_x, p_y). \quad (5.13)$$

$$\langle \eta^{v}_{\alpha\beta}\eta^{d}_{\alpha'\beta'}\rangle = \int_{-\pi}^{\pi} \frac{dp_x}{2\pi} \int_{-\pi}^{\pi} \frac{dp_x}{2\pi} \exp\,[i(\alpha - \alpha')p_x + i(\beta - \beta')p_y]$$

$$\times V_{27}(p_x, p_y) \,/\, L(p_x, p_y). \quad (5.14)$$

$$\langle \eta^{h}_{\alpha\beta}\eta^{d}_{\alpha'\beta'}\rangle = \int_{-\pi}^{\pi} \frac{dp_x}{2\pi} \int_{-\pi}^{\pi} \frac{dp_y}{2\pi} \exp\,[i(\alpha - \alpha')p_x + i(\beta - \beta')p_y]$$

$$\times V_{29}(p_x, p_y) \,/\, L(p_x, p_y). \quad (5.15)$$

$$\langle \eta^{v\dagger}_{\alpha\beta}\eta^{v\dagger}_{\alpha'\beta'}\rangle = \int_{-\pi}^{\pi} \frac{dp_x}{2\pi} \int_{-\pi}^{\pi} \frac{dp_x}{2\pi} \exp\,[i(\alpha' - \alpha)p_x + i(\beta' - \beta)p_y]$$

$$\times V_{31}(p_x, p_y) \,/\, L(p_x, p_y). \quad (5.16)$$

$$\langle \eta^{v}_{\alpha\beta}\eta^{v}_{\alpha'\beta'}\rangle = \int_{-\pi}^{\pi} \frac{dp_x}{2\pi} \int_{-\pi}^{\pi} \frac{dp_y}{2\pi} \exp\,[i(\alpha - \alpha')p_x + i(\beta - \beta')p_y]$$

$$\times V_{32}(p_x, p_y) \,/\, L(p_x, p_y). \quad (5.17)$$

$$\langle \eta^{h\dagger}_{\alpha\beta}\eta^{h\dagger}_{\alpha'\beta'}\rangle = \int_{-\pi}^{\pi} \frac{dp_x}{2\pi} \int_{-\pi}^{\pi} \frac{dp_y}{2\pi} \exp\,[i(\alpha' - \alpha)p_x + i(\beta' - \beta)p_y]$$

$$\times V_{33}(p_x, p_y) \,/\, L(p_x, p_y). \quad (5.18)$$

$$\langle \eta^{h}_{\alpha\beta}\eta^{h}_{\alpha'\beta'}\rangle = \int_{-\pi}^{\pi} \frac{dp_x}{2\pi} \int_{-\pi}^{\pi} \frac{dp_y}{2\pi} \exp\,[i(\alpha - \alpha')p_x + i(\beta - \beta')p_y]$$

$$\times V_{34}(p_x, p_y) \,/\, L(p_x, p_y). \quad (5.19)$$

$$\langle \eta^{d\dagger}_{\alpha\beta}\eta^{d\dagger}_{\alpha'\beta'}\rangle = \int_{-\pi}^{\pi} \frac{dp_x}{2\pi} \int_{-\pi}^{\pi} \frac{dp_y}{2\pi} \exp\,[i(\alpha' - \alpha)p_x + i(\beta' - \beta)p_y]$$

$$\times V_{35}(p_x, p_y) \,/\, L(p_x, p_y). \quad (5.20)$$

$$\langle \eta^{d}_{\alpha\beta}\eta^{d}_{\alpha'\beta'}\rangle = \int_{-\pi}^{\pi} \frac{dp_x}{2\pi} \int_{-\pi}^{\pi} \frac{dp_y}{2\pi} \exp\,[i(\alpha - \alpha')p_x + i(\beta - \beta')p_y]$$

$$\times V_{36}(p_x, p_y) \,/\, L(p_x, p_y). \quad (5.21)$$

These are useful formulas in the pseudo-free 32 vertex model.

VI. SPIN CORRELATIONS

This section calculates a spin-spin correlation function in the triangular Ising model using the method outlined in II. This method generalizes to the calculation of the vacuum expectation of an arbitrary product of spins in a relatively straight forward way, although the answer is, in general, cumbersome (a Pfaffian of large order). The formulas in Sec. V are the essential ingredients. Consider $\langle \sigma_{\alpha\beta}\sigma_{\alpha\beta+m}\rangle$, i.e. two spins in the same vertical column of Fig. 1a. This is expressible in terms of anticommuting variables as

$$\langle \sigma_{\alpha\beta}\sigma_{\alpha\beta+m}\rangle = \langle [z_v + (1 - z_v^2)\eta^{v\dagger}_{\alpha\beta}\eta^{v}_{\alpha\beta+1}][z_v + (1 - z_v^2)\eta^{v\dagger}_{\alpha\beta+1}\eta^{v}_{\alpha\beta+2}] \cdots$$

$$[z_v + (1 - z_v^2)\eta^{v\dagger}_{\alpha\beta+m-1}\eta^{v}_{\alpha\beta+m}]\rangle. \qquad (6.1)$$

One can choose $\alpha = \beta = 0$ because of translational invariance.

Define the $2m \times 2m$ antisymmetric matrix, M, by

$$M_{2i-1,\ 2j-1} = \langle \eta^{v\dagger}_{0,i-1}\eta^{v\dagger}_{0,j-1}\rangle\ (1 - z_v^2)\ , \qquad (6.2)$$

$$M_{2i,2j} = \langle \eta^{v}_{0,i}\eta^{v}_{0,j}\rangle(1 - z_v^2)\ ,$$

$$M_{2i-1,2j} = z_v\ \delta_{ij} + (1 - z_v^2)\langle \eta^{v\dagger}_{0,i-1}\eta^{v}_{0,j}\rangle.$$

Then

$$\langle \sigma_{\alpha\beta}\sigma_{\alpha\beta+m}\rangle = \text{Pf } M\ . \qquad (6.3)$$

In Eq. (6.2) i and j go from 1 to m. The three correlations needed are give in Eqs. (5.16), (5.17), and (5.1), with the parameter values of Eqs. (2.6) and (2.9).

The correlation, $\langle\sigma\sigma'\rangle$, on the hexangonal lattice can also be calculated. Again, it is a partition function on a defective

lattice (see section VI of paper II). Dual (disorder) variables must be used. Recall that this means polygons are drawn around regions of up and down spin. To calculate $\langle\sigma\sigma'\rangle$ draw a line on the hexangonal lattice connecting σ to σ'. This line intersects certain bonds on the dual (triangular) lattice. To obtain the correlation as a defective partition function, change the sign of these bond weights. This means that a minus sign results, as it should, whenever a polygon encloses one spin but not the other, i.e. when one spin is in a region of up spin and the other is in a region of down spin. Such a partition function can be expressed in terms of anticommuting variable correlations using a similar technique as used in obtaining Eq. (II. 6.2). Again, this method generalizes to the case of an arbitrary product of spins.

ACKNOWLEDGMENTS

I thank Harry Morrison for reading the manuscript and making useful suggestions. I thank Korkut Bardakci and Harry Morrison for encouragement.

REFERENCES

1. S. Samuel, The Use of Anticommuting Integrals in Statistical Mechanics I, LBL preprint 8217, September 1978. Equations and Figures referred to in this paper are prefaced by an I.
2. S. Samuel, The Use of Anticommuting Integrals in Statistical Mechanics II, LBL preprint 8300, October 1978. Equations and figures referred to in this paper are prefaced by a II.
3. B. B. van der Waerden, Z. Physik 118, 473 (1941). This is reviewed in I where a pedagogical set of references can be found.
4. H. S. Green and C. A. Hurst, Order-Disorder Theory, edited by I. Preigoine (Interscience, New York, 1964). See Sec. 5.3.
5. C. Fan and F. Y. Wu, Phys, Rev. B2, 723 (1970).
6. I have carried out this proof but omit it to keep this paper as short as possible.
7. G. H. Wannier, Phys. Rev. 79, 357 (1950). G. F. Newell, Phys. Rev. 79, 876 (1950). H. N. V. Temperley, Proc. Roy. Soc. (London) A 202, 202 (1950). R. M. F. Houtappel, Physica 16, 425 (1950). See also reference 4, chapter 5.

Figure 1. (a) The square lattice with one diagonal. (b) The triangular lattice. (c) The hexangonal lattice. Figure (b) is obtained from Fig. (a) by rotating the vertical lines counterclockwise by roughly 45°.

Figure 2. The Bloch wall operators of Eq. (2.3). These are (a) the horizontal Bloch wall operator, (b) The vertical Bloch wall operator, and (c) The diagonal Bloch wall operator. The corresponding Boltzmann factors are also indicated.

Figure 3. The corner operators of Eq. (2.4).

Figure 4. Intersection minus signs. A non self-intersecting polygon has no minus signs due to reording of anticommuting variables. When self-intersections occur, one must use the pasting construction of Fig. I. 16. This results in a minus sign for configuration (xviii) as Fig. (a) indicates. Configurations (xvii), (xix), (xxiv), (xxvi), (xxviii), and (xxx) are similar to Fig. (a) and have a minus sign. Figure (b), Fig. (c), and Fig. (d) show why minus signs result in configurations (xxi), (xxiii), and (xxxii).

Figure 5. The miniature dimer problem. For clarity the bonds have been drawn on four separate figures. One should take the bonds in Figs. (b), (c), and (d) and attach them to the "o"'s and "x"'s in Fig.(a) to obtain the miniature dimer problem. The upper left, middle left, lower left, upper right, middle right, and lower right sites respectively stand for the vertical (s,t), the horizontal (s,t), the diagonal (s,t), the vertical (-s, -t), the

horizontal (-s, -t), and the diagonal (-s, -t) variables. The bond weights are indicated in the figure.

Figure 6. The superbonds used to calculate $\langle a^v_{st} a^{v\dagger}_{st} \rangle$. The weight of the superbond is unity.

Figure 7. The symbolic representation of Eq. (4.1). Type 1 terms involve the $d(p_x, p_y)$ and $d(p_x, -p_y)$ bonds shown on the right. After bonds connecting to diagonal sites are erased, the free-fermion model results, and one needs $\langle a^v_{st} a^{v\dagger}_{st} \rangle$ for the free-fermion model as shown on the left.

Figure 8. The super bonds used to calculate type 2 terms in $\langle a^v_{st} a^{v\dagger}_{st} \rangle$. When two bonds are used from Figs. 5c and 5d two sites besides the vertical (s, t) sites get covered. The numbers in the upper left hand corners indicate the boxes of table 2 containing these sites and bonds. What results are MMDP's with two superbonds. The superbonds are shown here. There are nine different possibilities. The C_i factor is due to the bonds used from Figs. 5c and 5d as well as the $d(p_x, p_y)$ and $d(-p_x, -p_y)$ bonds. The C_i are given in Eq. (3.12). The F_i factor is the weight of the coverings of the MMDP. They can be found in table 3.

Figure 9. The superbonds used to calculate type 3 terms in $\langle a^v_{st} a^{v\dagger}_{st} \rangle$. When four bonds are used from Figs. 5c and 5d, four sites get covered in addition to the vertical (s, t) sites. The numbers in the upper left hand corners indicate the boxes of table 3 containing these sites.

What results are MMDP's with three superbonds. The superbonds are shown here. The E_i factors are due to the bonds from Figs. 5c and 5d and are given in the corresponding box of table 3. The easily calculated covering weight is the second factor $[h(-p_x), h(p_x), v(-p_y),$ etc.]. Figures (d) and (e) have no coverings, hence the zero.

Table 1. The thirty-two possible configurations which may occur. After the Bloch wall Boltzmann factors have been extracted their weights are (i) $[b_h b_v b_d]$ +
$[(-a_1a_3 - a_2a_4)b_d + (-b_1b_3 - b_2b_4)b_h + (-c_1c_3 - c_2c_4)b_v]$ +
$[a_1b_2c_4 - a_1b_3c_3 - a_2b_1c_4 - a_2b_4c_3 + a_3b_4c_2 - a_3b_1c_1 - a_4b_3c_2 - a_4b_2c_1]$,

(ii) $[b_h b_d] + [-c_1c_3 - c_2c_4]$,

(iii) $[b_v b_d] + [-b_1b_3 - b_2b_4]$,

(iv) $[b_h b_v] + [-a_1a_3 - a_2a_4]$,

(v) $[a_1 b_d] + [b_1c_1 - b_4c_2]$,

(vi) $[a_2 b_d] + [b_3c_2 + b_2c_1]$,

(vii) $[a_3 b_d] + [b_3c_3 - b_2c_4]$,

(viii) $[a_4 b_d] + [b_1c_4 + b_4c_3]$,

(ix) $[b_1 b_h] + [a_1c_3 + a_4c_2]$,

(x) $[b_2 b_h] + [a_2c_3 - a_3c_2]$,

(xi) $[b_3 b_h] + [a_3c_1 + a_2c_4]$,

(xii) $[b_4 b_h] + [a_4c_3 - a_1c_4]$,

(xiii) $[c_1 b_v] + [a_1b_3 + a_2b_4]$,

(xiv) $[c_2 b_v] + [a_2b_1 - a_1b_2]$,

(xv) $[c_3 b_v] + [a_3b_1 + a_4b_2]$,

(xvi) $[c_4 b_v] + [a_4 b_3 - a_3 b_4]$,

(xvii) $[-b_v]$,

(xviii) $[-b_h]$,

(xix) $[-b_d]$,

(xx) $[a_3]$,

(xxi) $[-a_4]$,

(xxii) $[a_1]$,

(xxiii) $[-a_2]$,

(xxiv) $[-b_3]$,

(xxv) $[b_4]$,

(xxvi) $[-b_1]$,

(xxvii) $[b_2]$,

(xxviii) $[-c_3]$,

(xxix) $[c_4]$,

(xxx) $[-c_3]$,

(xxxi) $[c_2]$,

(xxxii) $[-1]$.

Table 2. The A_i and B_i values. Column 1 shows the sixteen non-zero momentum space anticommuting variable correlations of the free-fermion model. For example, box 1 is $Z\langle a^v_{st} a^{v\dagger}_{st}\rangle$, box 2 is $Z\langle a^v_{-s-t} a^{v\dagger}_{-s-t}\rangle$, box 5 is $Z\langle a^{h\dagger}_{st} a^v_{st}\rangle$, etc. These correlations occur in two ways: when $d(-p_x, -p_y)$ and two bonds connecting to diagonal (s,t) sites from Figs. 5c and 5d are used or when $d(p_x, p_y)$ and two bonds connecting to diagonal $(-s, -t)$ sites are used. The former are shown in the second column with the corresponding weight or A_i value. The latter are shown in the third column with the corresponding B_i weight.

Table 3. The E_i and F_i values. There are 36 non-zero four point anticommuting variable correlations in the free-fermion model. These are shown in the first column. For example, in box 1 is

$$Z\langle a^v_{st} a^{v\dagger}_{st} a^v_{-s-t} a^{v\dagger}_{-s-t}\rangle = Z\langle a^v_{st} a^{v\dagger}_{st}\rangle\langle a^v_{-s-t} a^{v\dagger}_{-s-t}\rangle - Z\langle a^v_{st} a^v_{-s-t}\rangle\langle a^{v\dagger}_{st} a^{v\dagger}_{-s-t}\rangle \equiv F_1.$$

F_1 is the value of this correlation. In graphical language, it is the weight needed to cover the rest of the "o"'s and "x"'s. The E_i values are the bond weights needed to produce these correlations. Four bonds must be chosen from Figs. 5c and 5d, or two pairs from table 2. There are always four sets. For E_1 these are A_1 and B_2 bonds, A_2 and B_1 bonds, A_{13} and B_{14} bonds, or A_{14} and B_{13} bonds. This is how E_1 is calculated. The F_i are obtained by finding the covering of the corresponding modified miniature dimer problem. Boxes 2, 3, 4, 5, 8, and 9 have two coverings; the rest have only one.

When A_i and B_i are substituted into the E_i the following are obtained:

$$E_1 = (b_1 b_3 + b_2 b_4)^2$$

$$E_2 = E_5 = (b_1 c_4 + b_4 c_3)(b_3 c_2 + b_2 c_1)$$

$$E_3 = E_4 = (b_1 c_1 - b_4 c_2)(b_3 c_3 - b_2 c_4)$$

$$E_6 = (c_1 c_3 + c_2 c_4)^2$$

$$E_7 = (b_1 c_1 - b_4 c_2)^2$$

$$E_8 = E_9 = (b_1 b_3 + b_2 b_4)(c_1 c_3 + c_2 c_4)$$

$$E_{10} = (b_3 c_3 - b_2 c_4)^2$$

$$E_{11} = (b_3c_2 + b_2c_1)^2$$

$$E_{12} = (b_1c_4 + b_4c_3)^2$$

$$E_{13} = E_{19} = (b_1b_3 + b_2b_4)(b_4c_2 - b_1c_1)$$

$$E_{14} = E_{20} = (b_1b_3 + b_2b_4)(b_2c_4 - b_3c_3)$$

$$E_{15} = E_{21} = -(b_1b_3 + b_2b_4)(b_3c_2 + b_2c_1)$$

$$E_{16} = E_{22} = -(b_1b_3 + b_2b_4)(b_4c_3 + b_1c_4)$$

$$E_{17} = -E_{23} = (b_3c_2 + b_2c_1)(b_1c_1 - b_4c_2)$$

$$E_{18} = -E_{24} = (b_1c_4 + b_4c_3)(b_3c_3 - b_2c_4)$$

$$E_{25} = E_{31} = (b_4c_2 - b_1c_1)(c_1c_3 + c_2c_4)$$

$$E_{26} = E_{32} = (b_2c_4 - b_3c_3)(c_1c_3 + c_2c_4)$$

$$E_{27} = E_{33} = -(b_3c_2 + b_2c_1)(c_1c_3 + c_2c_4)$$

$$E_{28} = E_{34} = -(b_4c_3 + b_1c_4)(c_1c_3 + c_2c_4)$$

$$E_{29} = -E_{35} = (b_2c_4 - b_3c_3)(b_3c_2 + b_2c_1)$$

$$E_{30} = -E_{36} = (b_4c_2 - b_1c_1)(b_4c_3 + b_1c_4)$$

Table 4. The V_i values. In the boxes to the left are the correlation functions. For example, boxes 1, 3, 5, and 7 are $\langle a^v_{st} a^{v\dagger}_{st} \rangle$, $\langle a^h_{st} a^{h\dagger}_{st} \rangle$, $\langle a^d_{st} a^{d\dagger}_{st} \rangle$, and $\langle a^{h\dagger}_{st} a^v_{st} \rangle$. To the right are the V_i values of the MMDP's. For $i \leq 15$, $V_{2i}(p_x, p_y) \equiv V_{2i-1}(-p_x, -p_y)$ so that these boxes are not shown. Many of the V_i are obtained from other V_i's by one of the transformations of Eqs. (4.4)-(4.9), in which case the transformation is indicated. For example, V_3 is written in terms of V_1 by using transformation (i). In transforming, one must explicitly put in all the functional dependence on

the a_i, b_i, and c_i parameters, as well as the h,v, and d functions. This means that in obtaining V_3 from V_1, W_1, C_2, F_1, C_3, F_2, etc. must be expressed in terms of the a_i, b_i, c_i, h, v, and d. The symbols h, v, and d stand for $h(p_x)$ or $h(-p_x)$, $v(p_y)$ or $v(-p_y)$, and $d(p_x, p_y)$ or $d(-p_x, -p_y)$.

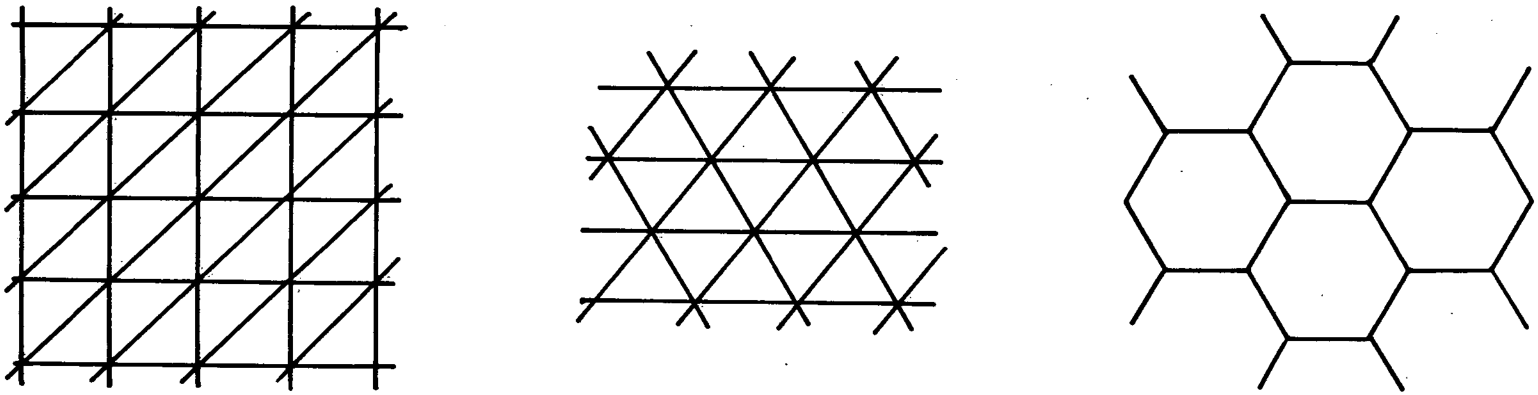

(a) (b) (c)

Fig. 1

XBL7811-12646

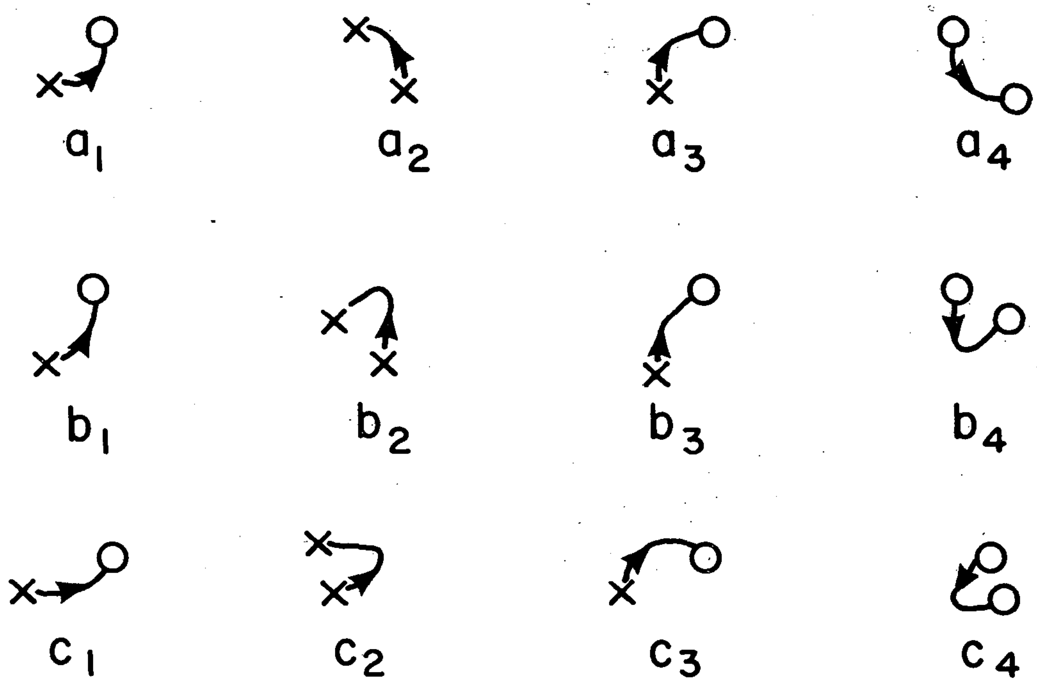

Fig. 3 XBL7811-12642

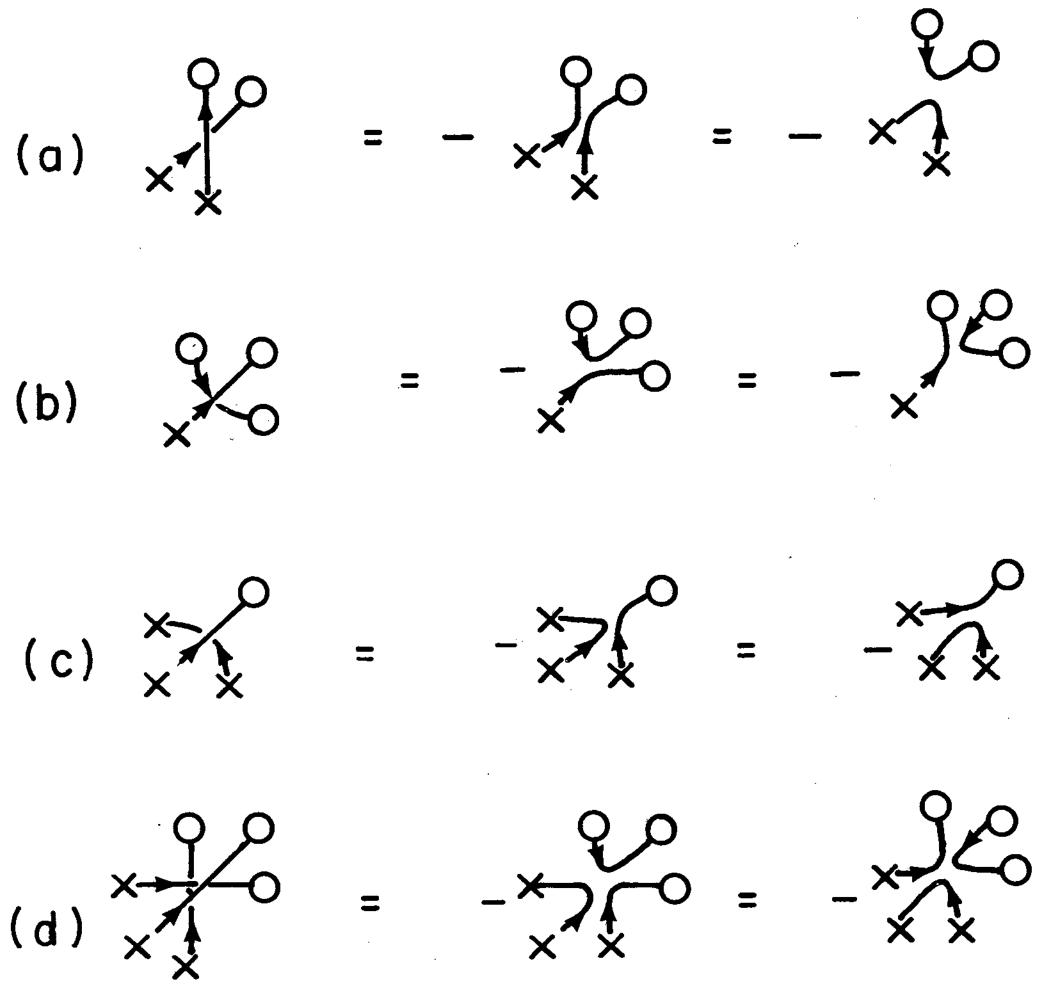

Fig. 4 XBL7811-12644

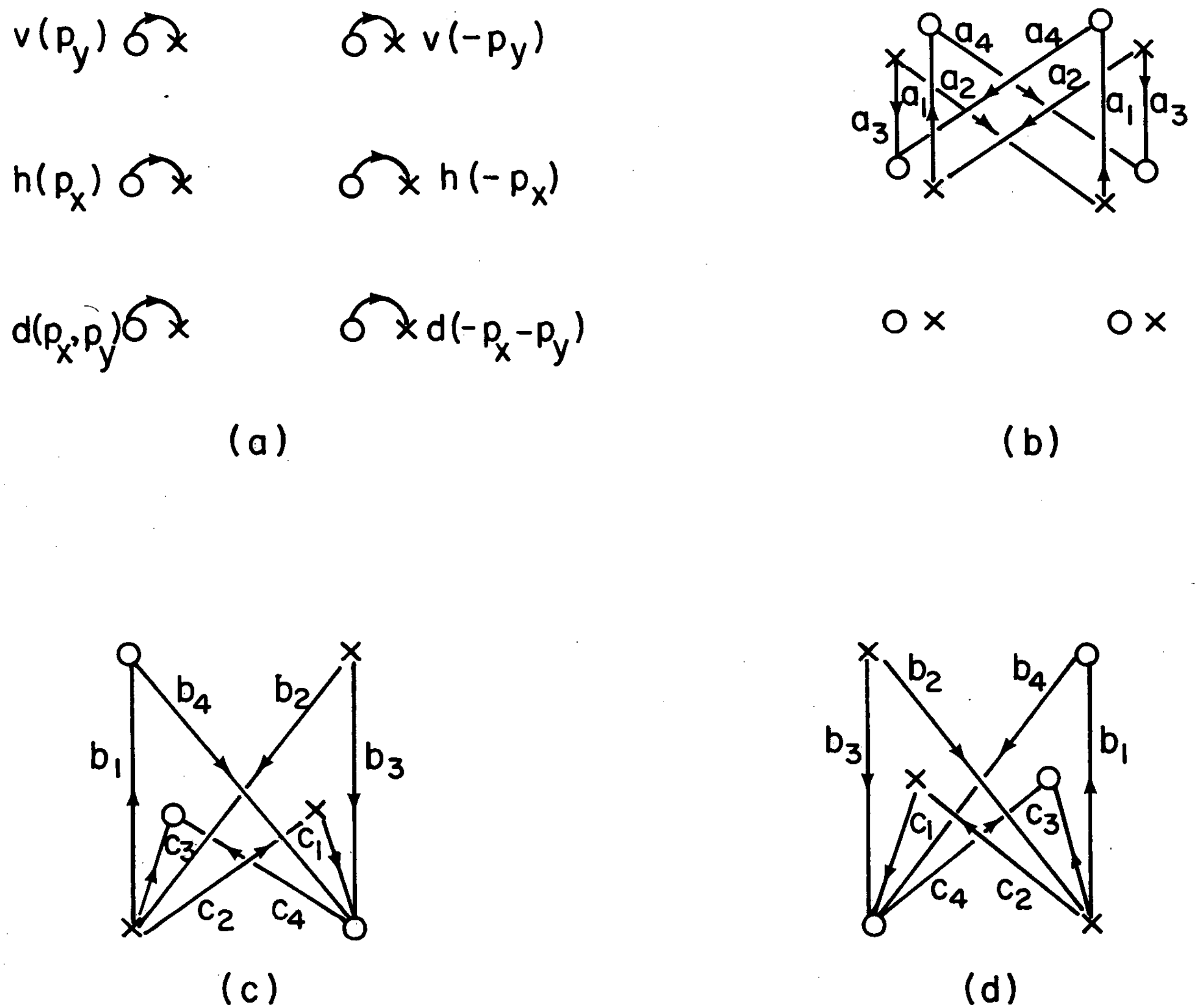

Fig. 5

XBL7811-12641

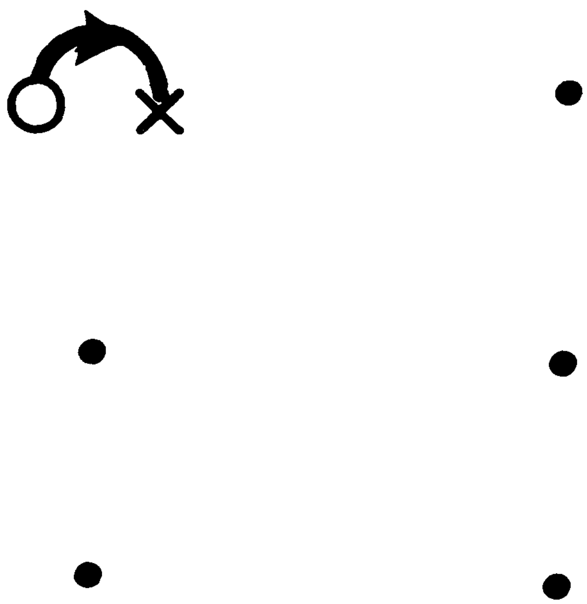

Fig. 6

XBL7811-12645

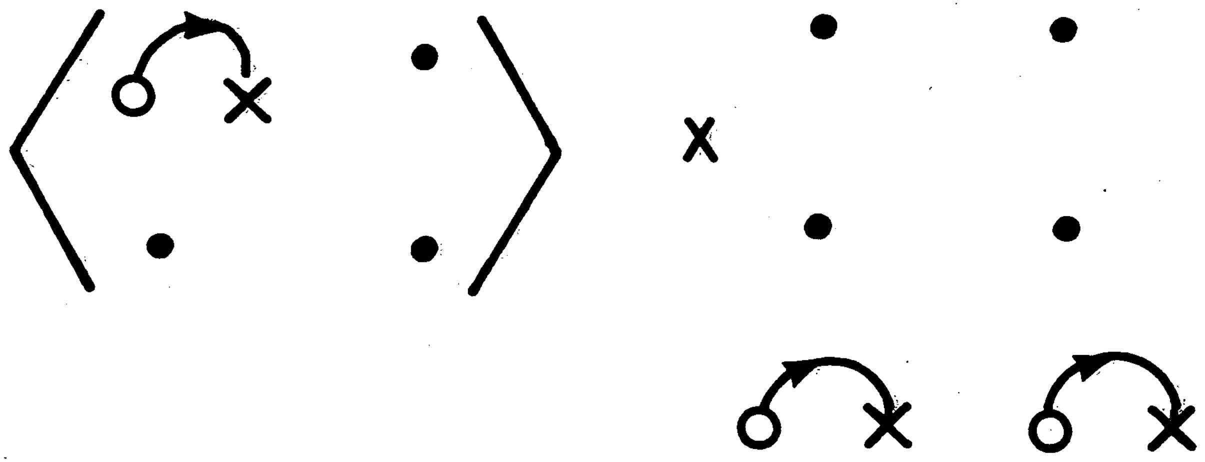

Fig. 7 XBL 7811-12657

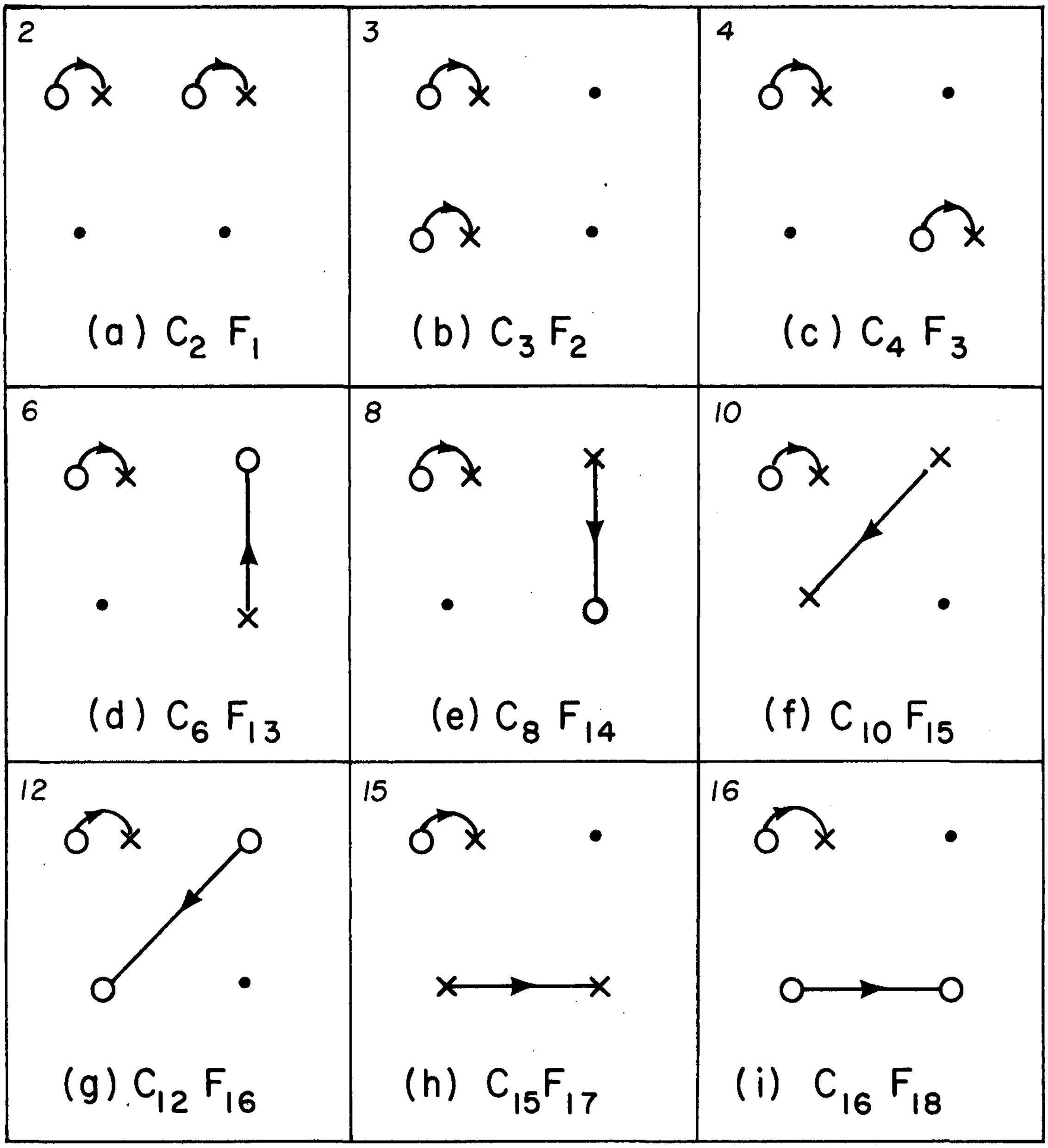

Fig. 8 XBL 7811-12640

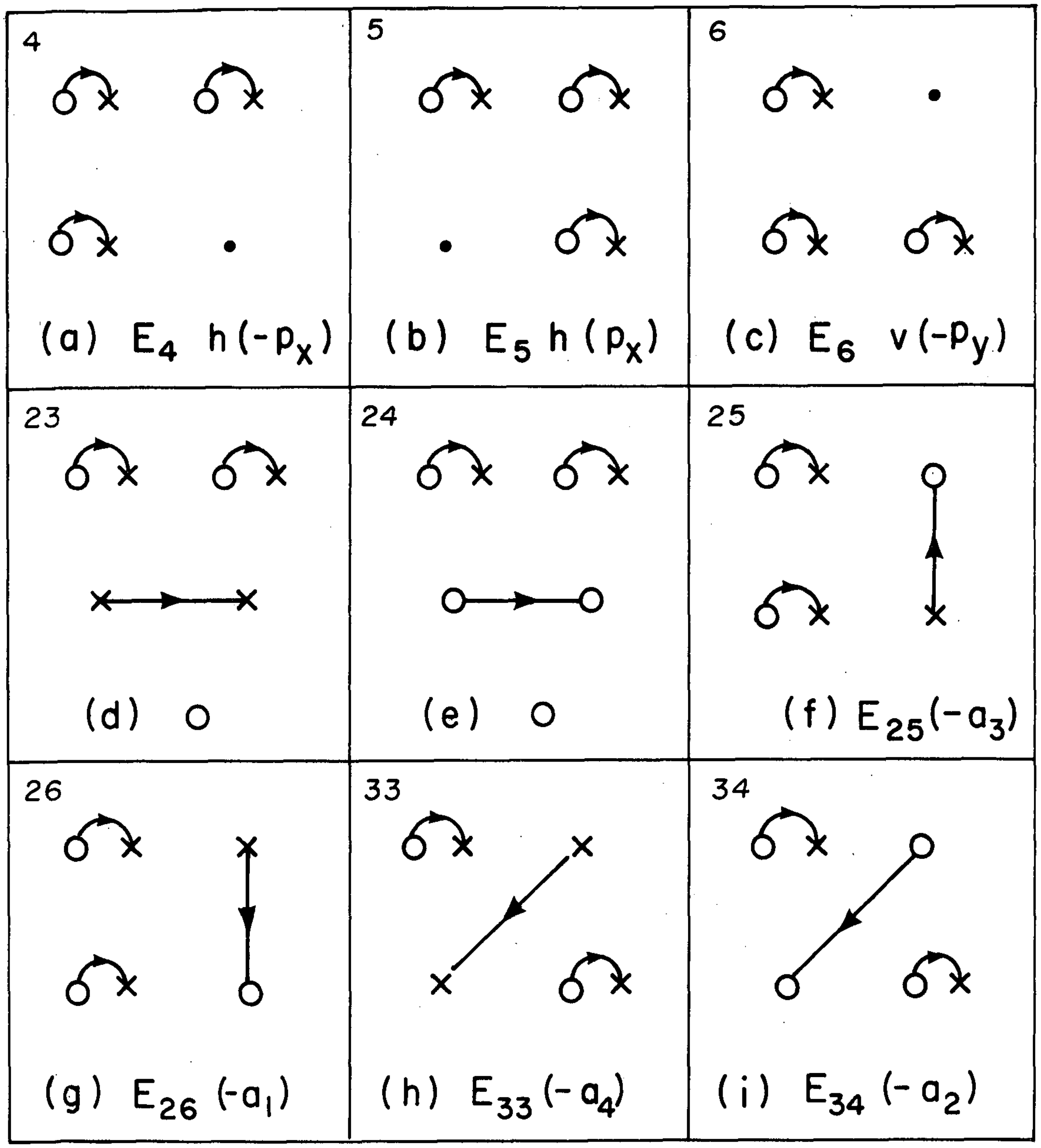

Fig. 9

XBL7811-12647

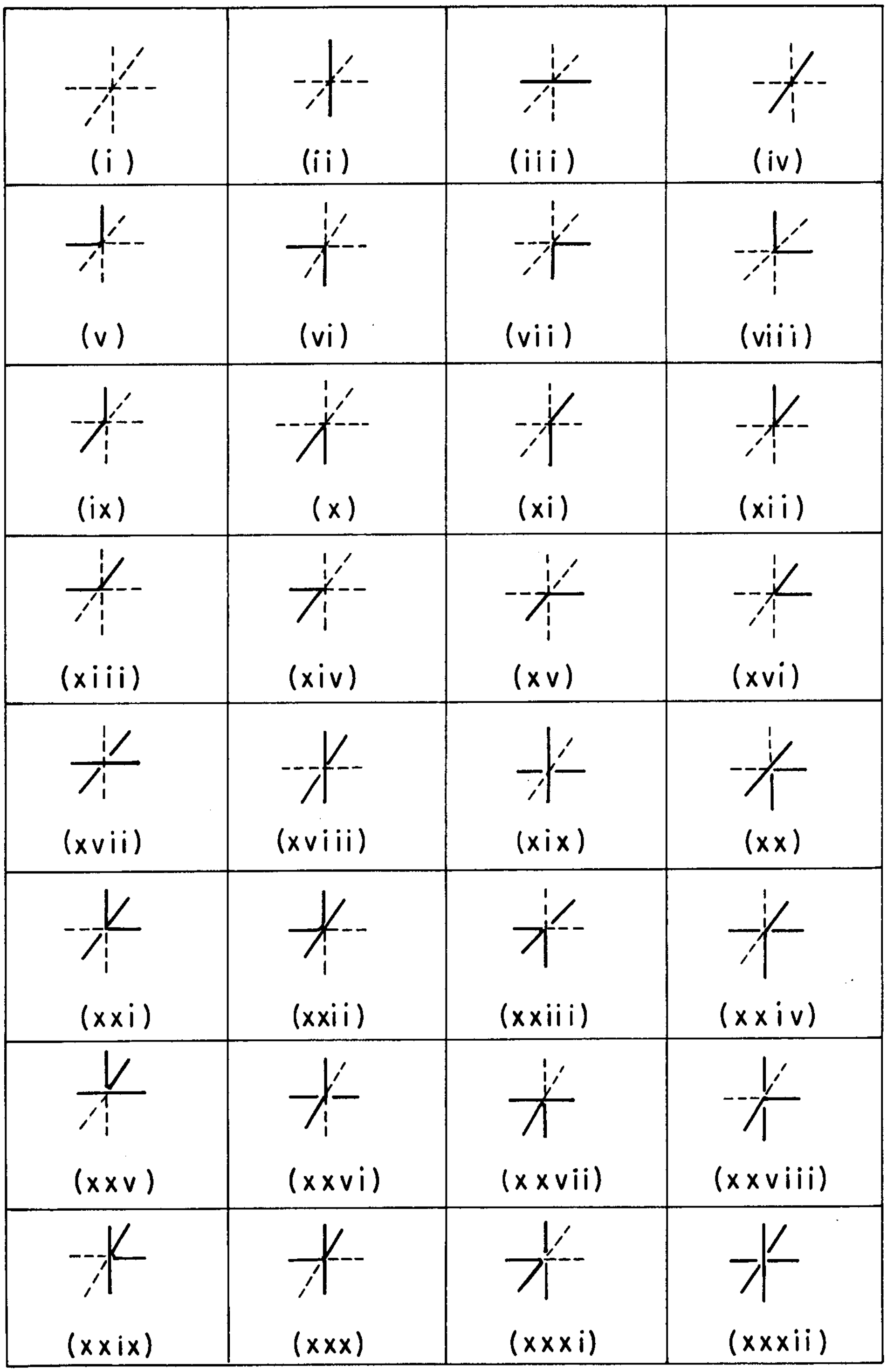

Table 1

XBL7811-12651

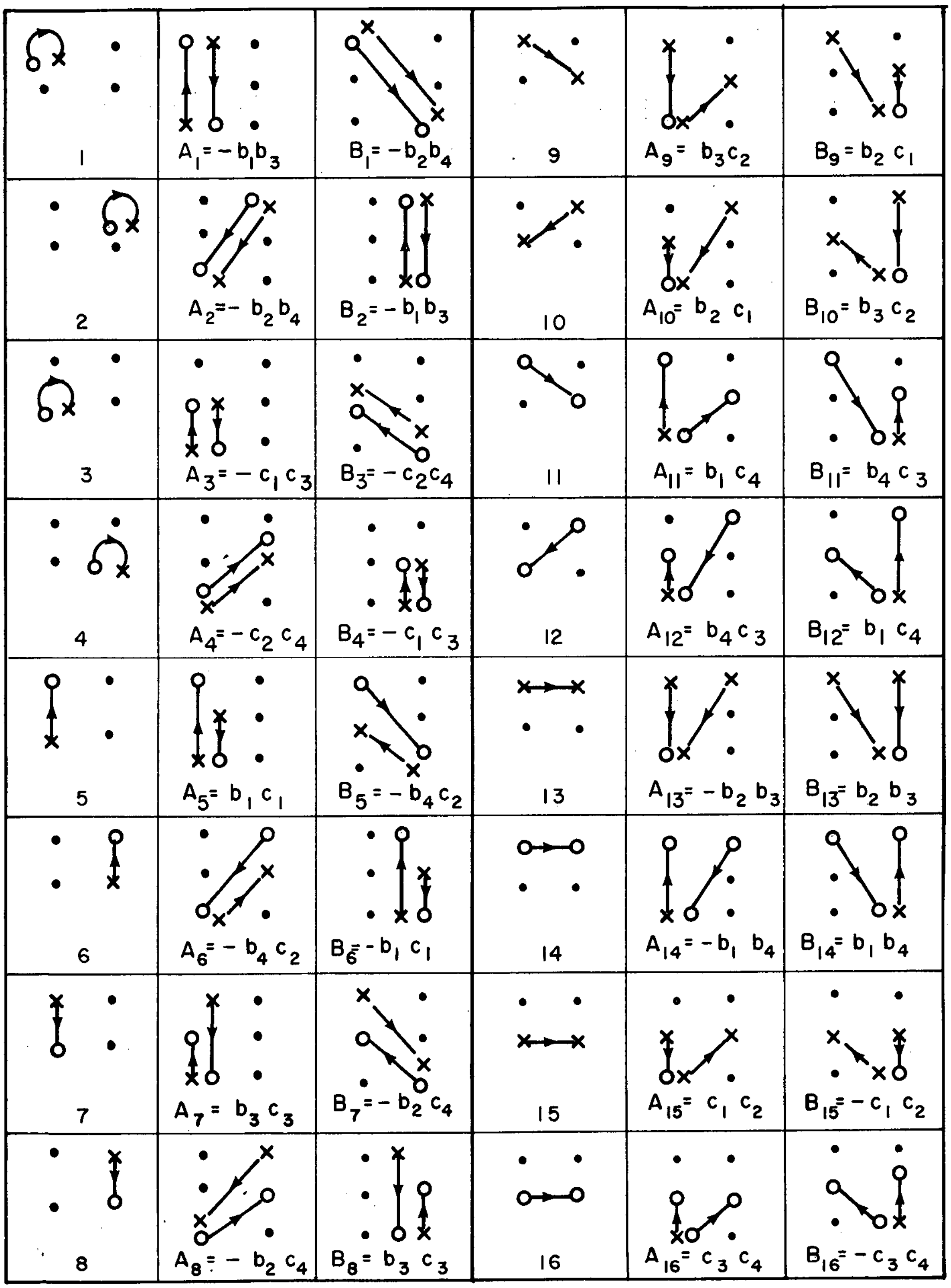

Table 2

XBL7811-12653

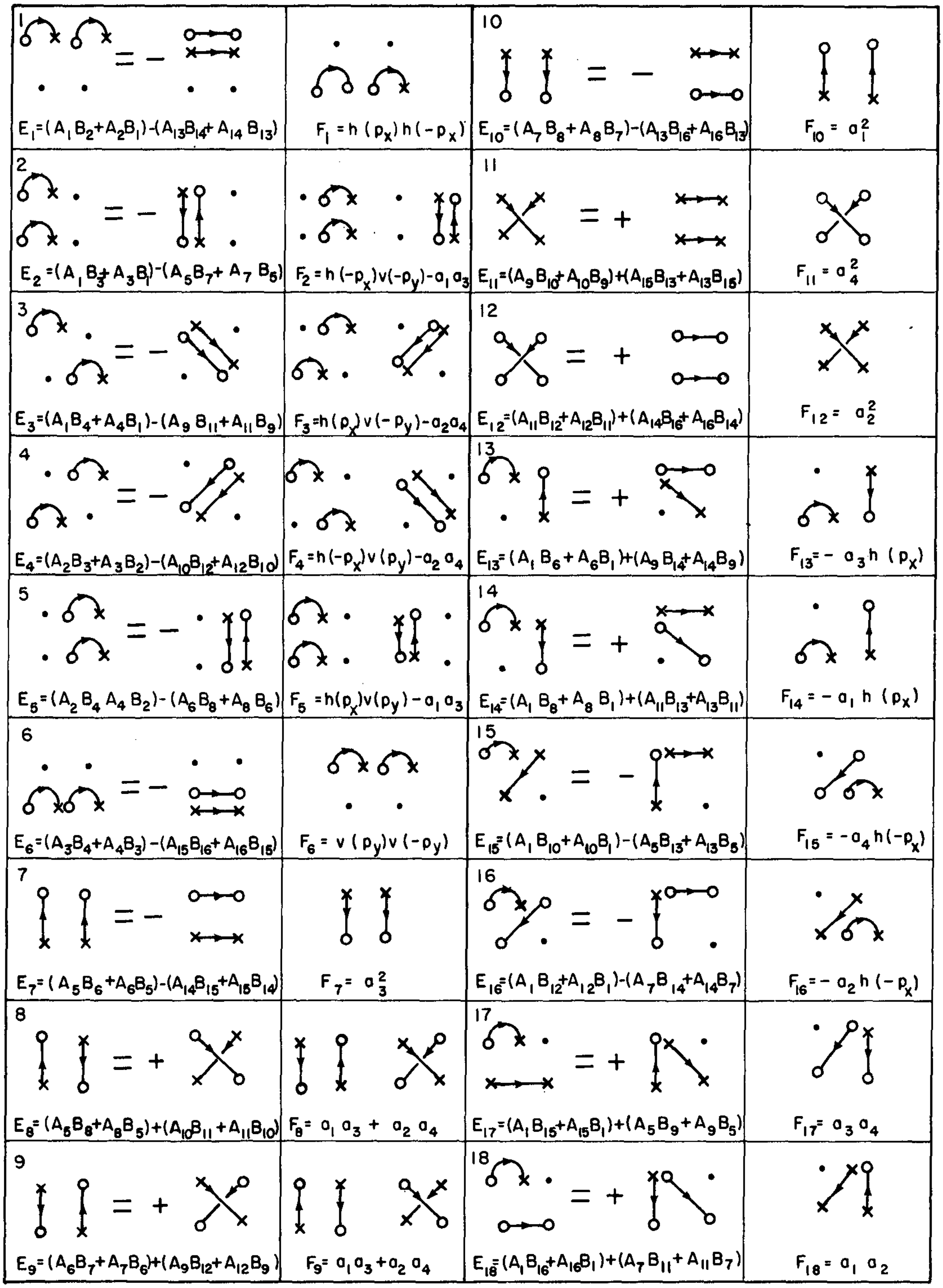

XBL7811-12654

Table 3

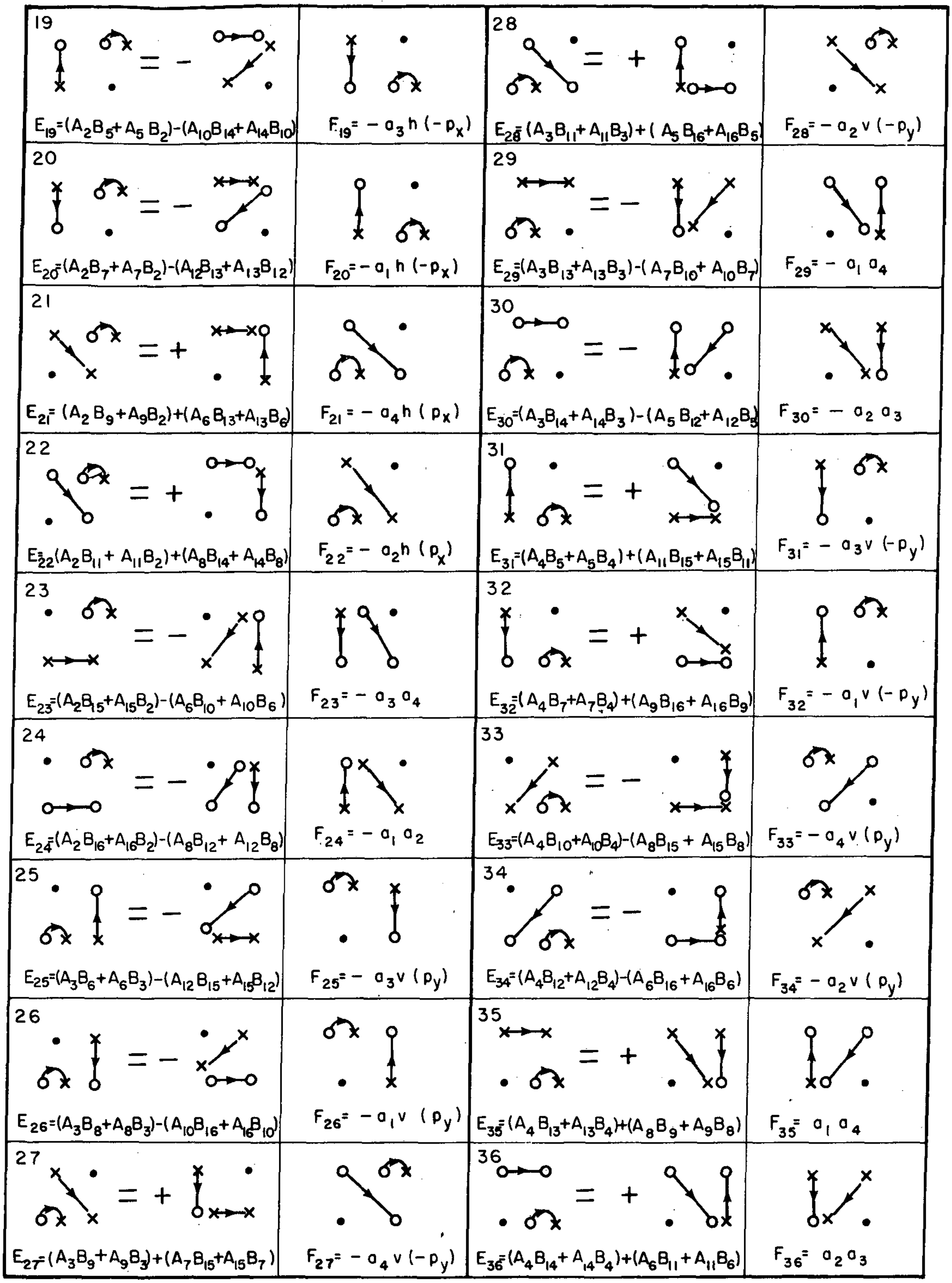

19	$E_{19}=(A_2B_5+A_5B_2)-(A_{10}B_{14}+A_{14}B_{10})$	$F_{19}=-a_3h(-p_x)$
20	$E_{20}=(A_2B_7+A_7B_2)-(A_{12}B_{13}+A_{13}B_{12})$	$F_{20}=-a_1h(-p_x)$
21	$E_{21}=(A_2B_9+A_9B_2)+(A_6B_{13}+A_{13}B_6)$	$F_{21}=-a_4h(p_x)$
22	$E_{22}=(A_2B_{11}+A_{11}B_2)+(A_8B_{14}+A_{14}B_8)$	$F_{22}=-a_2h(p_x)$
23	$E_{23}=(A_2B_{15}+A_{15}B_2)-(A_6B_{10}+A_{10}B_6)$	$F_{23}=-a_3a_4$
24	$E_{24}=(A_2B_{16}+A_{16}B_2)-(A_8B_{12}+A_{12}B_8)$	$F_{24}=-a_1a_2$
25	$E_{25}=(A_3B_6+A_6B_3)-(A_{12}B_{15}+A_{15}B_{12})$	$F_{25}=-a_3v(p_y)$
26	$E_{26}=(A_3B_8+A_8B_3)-(A_{10}B_{16}+A_{16}B_{10})$	$F_{26}=-a_1v(p_y)$
27	$E_{27}=(A_3B_9+A_9B_3)+(A_7B_{15}+A_{15}B_7)$	$F_{27}=-a_4v(-p_y)$
28	$E_{28}=(A_3B_{11}+A_{11}B_3)+(A_5B_{16}+A_{16}B_5)$	$F_{28}=-a_2v(-p_y)$
29	$E_{29}=(A_3B_{13}+A_{13}B_3)-(A_7B_{10}+A_{10}B_7)$	$F_{29}=-a_1a_4$
30	$E_{30}=(A_3B_{14}+A_{14}B_3)-(A_5B_{12}+A_{12}B_5)$	$F_{30}=-a_2a_3$
31	$E_{31}=(A_4B_5+A_5B_4)+(A_{11}B_{15}+A_{15}B_{11})$	$F_{31}=-a_3v(-p_y)$
32	$E_{32}=(A_4B_7+A_7B_4)+(A_9B_{16}+A_{16}B_9)$	$F_{32}=-a_1v(-p_y)$
33	$E_{33}=(A_4B_{10}+A_{10}B_4)-(A_8B_{15}+A_{15}B_8)$	$F_{33}=-a_4v(p_y)$
34	$E_{34}=(A_4B_{12}+A_{12}B_4)-(A_6B_{16}+A_{16}B_6)$	$F_{34}=-a_2v(p_y)$
35	$E_{35}=(A_4B_{13}+A_{13}B_4)+(A_8B_9+A_9B_8)$	$F_{35}=a_1a_4$
36	$E_{36}=(A_4B_{14}+A_{14}B_4)+(A_6B_{11}+A_{11}B_6)$	$F_{36}=a_2a_3$

Table 3 (continued) XBL 7811-12652

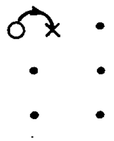 1	$V_1(v,h,d;a_1,a_2,a_3,a_4;b_1,b_2,b_3,b_4;c_1,c_2,c_3,c_4) = W_1 d(p_x,p_y)d(-p_x, -p_y)$ $+ C_2F_1 + C_3F_2 + C_4F_3 + C_6F_{13} + C_8F_{14} + C_{10}F_{15} + C_{12}F_{16} + C_{15}F_{17} + C_{16}F_{18}$ $+ E_4h(-p_x) + E_5h(p_x) + E_6v(-p_y) - E_{25}a_3 - E_{26}a_1 - E_{33}a_4 - E_{34}a_2$
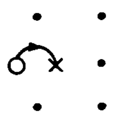 3	Transformation (i) applied to V_1 $V_3(v,h,d;a_1,a_2,a_3,a_4;b_1,b_2,b_3,b_4;c_1,c_2,c_3,c_4) = V_1(h,v,d;a_3, -a_2,a_1, -a_4;c_3, -c_2,c_1, -c_4;b_3, -b_2,b_1, -b_4)$
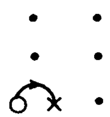 5	Transformation (iii) applied to V_1 $V_5(v,h,d;a_1,a_2,a_3,a_4;b_1,b_2,b_3,b_4;c_1,c_2,c_3,c_4) = V_1(d,h,v;c_1,c_2,c_3,c_4;b_3, -b_2,b_1, -b_4;a_1,a_2,a_3,a_4)$

Table 4

XBL 7811-12650

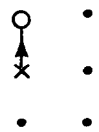 7	$V_7(v,h,d;a_1,a_2,a_3,a_4;b_1,b_2,b_3,b_4;c_1,c_2,c_3,c_4) = W_5 d(p_x,p_y)d(-p_x,-p_y)$ $+ C_2F_{19} + C_4F_{31} + C_6F_7 - C_7F_2 + C_8F_8 + C_9F_{17} - C_{12}F_{30} - C_{13}F_{15} + C_{16}F_{28}$, $- E_5a_3 + E_9a_3 + E_{10}a_1 - E_{20}h(-p_x) - E_{24}a_2 - E_{32}v(-p_y) + E_{35}a_4$
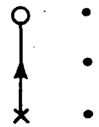 9	Transformation (ii) applied to V_7 $V_9(v,h,d;a_1,a_2,a_3,a_4;b_1,b_2,b_3,b_4;c_1,c_2,c_3,c_4) = V_7(v,d,h;b_1,b_2,b_3,b_4;a_1,a_2,a_3,a_4;c_3,-c_2,c_1,-c_4)$
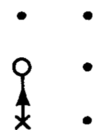 11	Transformation (iv) applied to V_7 $V_{11}(v,h,d;a_1,a_2,a_3,a_4;b_1,b_2,b_3,b_4;c_1,c_2,c_3,c_4) = V_7(h,d,v;c_3,-c_2,c_1,-c_4;a_3,-a_2,a_1,-a_4;b_1,b_2,b_3,b_4)$
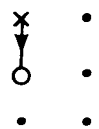 13	Transformation (i) applied to V_7 $V_{13}(v,h,d;a_1,a_2,a_3,a_4;b_1,b_2,b_3,b_4;c_1,c_2,c_3,c_4) = V_7(h,v,d;a_3,-a_2,a_1,-a_4;c_3,-c_2,c_1,-c_4;b_3,-b_2,b_1,-b_4)$
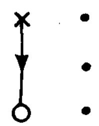 15	Transformation (v) applied to V_7 $V_{15}(v,h,d;a_1,a_2,a_3,a_4;b_1,b_2,b_3,b_4;c_1,c_2,c_3,c_4) = V_7(d,v,h;b_3,-b_2,b_1,-b_4;c_1,c_2,c_3,c_4;a_3,-a_2,a_1,-a_4)$
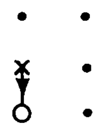 17	Transformation (iii) applied to V_7 $V_{17}(v,h,d;a_1,a_2,a_3,a_4;b_1,b_2,b_3,b_4;c_1,c_2,c_3,c_4) = V_7(d,h,v;c_1,c_2,c_3,c_4;b_3,-b_2,b_1,-b_4;a_1,a_2,a_3,a_4)$

Table 4 (continued)

XBL 7811 - 12649

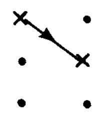 19	$V_{19}(v,h,d;a_1,a_2,a_3,a_4;b_1,b_2,b_3,b_4;c_1,c_2,c_3,c_4) = W_9 d(p_x, p_y)d(-p_x, -p_y)$ $+ C_2F_{21} + C_3F_{27} + C_{15}F_{17} + C_8F_{35} + C_{10}F_{11} - C_{11}F_3 + C_{12}F_9 + C_{14}F_{13} + C_{16}F_{32}$ $- E_4a_4 + E_8a_4 + E_{12}a_4 - E_{22}h(p_x) - E_{24}a_1 - E_{28}v(-p_y) - E_{30}a_3$
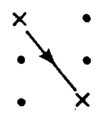 21	Transformation (ii) applied to V_{19} $V_{21}(v,h,d;a_1,a_2,a_3,a_4;b_1,b_2,b_3,b_4;c_1,c_2,c_3,c_4) = V_{19}(v,d,h;b_1,b_2,b_3,b_4;a_1,a_2,a_3,a_4;c_3, -c_2, c_1, -c_4)$
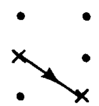 23	Transformation (iv) applied to V_{19} $V_{23}(v,h,d;a_1,a_2,a_3,a_4;b_1,b_2,b_3,b_4;c_1,c_2,c_3,c_4) = V_{19}(h,d,v;c_3, -c_2,c_1, -c_4;a_3, -a_2,a_1, -a_4;b_1,b_2,b_3,b_4)$
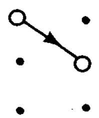 25	$V_{25}(v,h,d;a_1,a_2,a_3,a_4;b_1,b_2,b_3,b_4;c_1,c_2,c_3,c_4) = W_{11}d(p_x, p_y)d(-p_x,-p_y)$ $+ C_2F_{22} + C_3F_{28} + C_6F_{36} + C_7F_{18} - C_9F_3 + C_{10}F_8 + C_{12}F_{12} + C_{13}F_{14} + C_{15}F_{31}$ $- E_4a_2 + E_9a_2 + E_{11}a_4 - E_{21}h(p_x) - E_{23}a_3 - E_{27}v(-p_y) - E_{29}a_1$
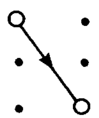 27	Transformation (ii) applied to V_{25} $V_{27}(v,h,d;a_1,a_2,a_3,a_4;b_1,b_2,b_3,b_4;c_1,c_2,c_3,c_4) = V_{25}(v,d,h;b_1,b_2,b_3,b_4;a_1,a_2,a_3,a_4;c_3, -c_2,c_1, -c_4)$
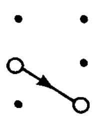 29	Transformation (iv) applied to V_{25} $V_{29}(v,h,d;a_1,a_2,a_3,a_4;b_1,b_2,b_3,b_4;c_1,c_2,c_3,c_4) = V_{25}(c_3, -c_2,c_1, -c_4;a_3, -a_2,a_1, -a_4;b_1,b_2,b_3b_4)$

Table 4 (continued)

XBL7811-12651A

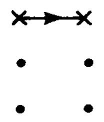 31	$V_{31}(v,h,d;a_1,a_2,a_3,a_4;b_1,b_2,b_3,b_4;c_1,c_2,c_3,c_4) = W_{13}d(p_x, p_y)d(-p_x, -p_y)$ $+ C_3F_{29} + C_4F_{35} - C_5F_{15} + C_6F_{21} + C_{11}F_{14} - C_{12}F_{20} - C_{14}F_1 + C_{15}F_{11} - C_{16}F_{10}$ $- E_{25}a_4 - E_{28}a_1 - E_{30}h(-p_x) + E_{31}a_4 + E_{34}a_1 - E_{36}h(p_x)$
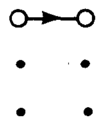 32	$V_{32}(v,h,d;a_1,a_2,a_3,a_4;b_1,b_2,b_3,b_4,c_1,c_2,c_3,c_4) = W_{14}d(p_x, p_y)d(-p_x, -p_y)$ $+ C_3F_{30} + C_4F_{36} - C_7F_{16} + C_8F_{22} + C_9F_{13} - C_{10}F_{19} - C_{13}F_1 - C_{15}F_7 + C_{16}F_{12}$ $- E_{26}a_2 - E_{27}a_3 - E_{29}h(-p_x) + E_{32}a_2 + E_{33}a_3 - E_{35}h(p_x)$
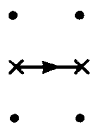 33	Transformation (i) applied to V_{31} $V_{33}(v,h,d;a_1,a_2,a_3,a_4;b_1,b_2,b_3,b_4;c_1,c_2,c_3,c_4) = V_{31}(h,v,d;a_3, -a_2,a_1, -a_4;c_3,-c_2,c_1, -c_4;b_3, -b_2,b_1, -b_4)$
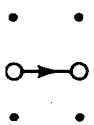 34	Transformation (i) applied to V_{32} $V_{34}(v,h,d;a_1,a_2,a_3,a_4;b_1,b_2,b_3,b_4;c_1,c_2,c_3,c_4) = V_{32}(h,v,d;a_3, -a_2,a_1, -a_4;c_3, -c_2,c_1, -c_4;b_3, -b_2,b_1, -b_4)$
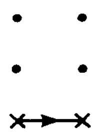 35	Transformation (iii) applied to V_{31} $V_{35}(v,h,d;a_1,a_2,a_3,a_4;b_1,b_2,b_3,b_4;c_1,c_2,c_3,c_4) = V_{31}(d,h,v;c_1,c_2,c_3,c_4;b_3, -b_2,b_1, -b_4;a_1,a_2,a_3,a_4)$
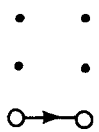 36	Transformation (iii) applied to V_{32} $V_{36}(v,h,d;a_1,a_2,a_3,a_4;b_1,b_2,b_3,b_4;c_1,c_2,c_3,c_4) = V_{32}(d,h,v;c_1,c_2,c_3,c_4;b_3, -b_2,b_1, -b_4;a_1,a_2,a_3,a_4)$

XBL7811-12648

Table 4 (continued)

This report was done with support from the Department of Energy. Any conclusions or opinions expressed in this report represent solely those of the author(s) and not necessarily those of The Regents of the University of California, the Lawrence Berkeley Laboratory or the Department of Energy.

TECHNICAL INFORMATION DEPARTMENT
LAWRENCE BERKELEY LABORATORY
UNIVERSITY OF CALIFORNIA
BERKELEY, CALIFORNIA 94720